Distribution Agreement

In presenting this thesis as a partial fulfillment of the requirements for a degree from Emory University, I hereby grant to Emory University and its agents the non-exclusive license to archive, make accessible, and display my thesis in whole or in part in all forms of media, now or hereafter know, including display on the World Wide Web. I understand that I may select some access restrictions as part of the online submission of this thesis. I retain all ownership rights to the copyright of the thesis. I also retain the right to use in future works (such as articles or books) all or part of this thesis.

Timothy J. Libecap 2016 April 12, 2016

Stereological Analysis of Prefrontal GABAergic Interneurons following Perinatal Hippocampal Lesion in Rhesus monkeys

by

Timothy J. Libecap

Dr. Hillary Rodman

Adviser

Neuroscience and Behavioral Biology

Dr. Hillary Rodman Adviser

Dr. Jocelyne Bachevalier Committee Member

Dr. Yoland Smith Committee Member

Dr. Michael Treadway Committee Member

2016

Stereological Analysis of Prefrontal GABAergic Interneurons following Neonatal Hippocampal Lesion in Rhesus monkeys

By Timothy J. Libecap

Dr. Hillary Rodman
Adviser

An abstract of
a thesis submitted to the Faculty of Emory College of Arts and Sciences
of Emory University in partial fulfillment
of the requirements of the degree of
Bachelor of Science with Honors

Neuroscience and Behavioral Biology

2016

Abstract

Stereological Analysis of Prefrontal GABAergic Interneurons following Neonatal Hippocampal Lesion in Rhesus monkeys

By Timothy J. Libecap

GABA is the primary inhibitory neurotransmitter in the mammalian brain. Under normal working circumstances, GABA plays a fundamental role in the dorsolateral prefrontal cortex (dlPFC). In particular, the parvalbumin class of GABA interneurons is involved in sustaining the normal neuron signaling that maintains proper functionality. The dlPFC is a brain region responsible for executive functioning and undergoes a protracted development. Disruption to its development may play a role in working memory impairment and other cognitive deficits associated with neurodevelopmental disorders including schizophrenia. Further, the hippocampus is a region in the medial temporal lobe that develops early in life and has been implicated in the development of the dlPFC as a result of their synaptic connections. In our study, we used tissue harvested from four control and four experimental adult rhesus monkeys that sustained bilateral neonatal hippocampal lesions of varying degree in order to better understand the role of the hippocampus in the development of the dlPFC. Specifically, we analyzed the relative density of parvalbumin-immunoreactive GABAergic interneurons in Brodmann Area 46d of lesioned (Neo-H) and non-lesioned monkeys (Neo-C). We used immunohistochemistry, Giemsa counterstain, and principles of stereology to visualize and analyze the density of PV-labeled neurons. We found a significantly higher density of parvalbumin-positive neurons within the dlPFC of the Neo-H monkeys relative to the Neo-C monkeys, both between the left hemispheres of the two groups and across the groups when both hemispheres were considered together. These results were confirmed by estimations of total PV-positive neuron populations in area 46d. Moreover, a correlation analysis between the hippocampal volume reduction and PV-positive cell density demonstrated a strong positive correlation such that a more greatly reduced hippocampus corresponded with a greater density of PV-stained cells. Our results are consistent with functional connectivity and behavioral data taken from the same monkeys. These findings have implications for how early life lesions of the hippocampus may affect vulnerable structures and disrupt cognitive processing. This work suggests that structural analysis of lesion studies supplements behavioral data to support a more comprehensive understanding of complex circuitry underlying psychiatric disease etiology.

Keywords*: GABA, parvalbumin, frontal cortex, hippocampus, development, working memory, rhesus monkey, stereology*

Stereological Analysis of Prefrontal GABAergic Interneurons following Neonatal Hippocampal Lesion in Rhesus monkeys

Timothy J. Libecap

Dr. Hillary Rodman
Adviser

A thesis submitted to the Faculty of Emory College of Arts and Sciences
of Emory University in partial fulfillment
of the requirements of the degree of
Bachelor of Sciences with Honors

Neuroscience and Behavioral Biology

2016

Acknowledgements

I would like to thank everyone that supported me in my undergraduate research in the Rodman Lab over the past three years that have culminated in this Honors Thesis. I thank my parents, extended family, and friends Thomas Partin and Emily Moore for undying support and motivation. I also would like to thank Emory's SIRE and Undergraduate Research programs, specifically Dr. Jacob Shreckengost, Dr. Gillian Hue, and Dr. Folashade Alao, for supporting my work through various stipends and grants and for aiding in my development as an ethically-minded scientist. I would like to thank Dr. Lydia Soleil and Dean Joanne Brzinski of the Emory Scholars Program for supporting my Summer 2015 stipend as the Garland Richmond Excellence in Research Fellow. I would like to thank my Honors Committee, Dr. Jocelyne Bachevalier, Dr. Yoland Smith, and Dr. Michael Treadway, for their efforts as a part of this process and the intellectual support they provided. In addition I would like to thank Dr. Smith and Dr. Rosa Villalba for the resources and expertise they provided relating to principles of stereology as well as for substantive writing advice. I would also like to extend a special thanks to our collaborator Dr. Bachevalier, without who this project would not have been possible. I would like to thank the entire Rodman Lab, but especially Richard Chen and Austin Howley, for their efforts relating to the experimental setup and execution of this project. Most of all, I would like to extend a deep sense of gratitude to Dr. Hillary Rodman for her incredible devotion and support of me in all my lab and non-lab pursuits at Emory. Her motivation pushed me to excel during my time at Emory and I know that I would not have been nearly as successful without her guidance. Thanks to Dr. Rodman I discovered the joy of research and hope to continue as long as possible. For that, I will always be grateful.

Table of Contents:

Introduction ..... pg. 1
GABA and GABAergic neurons ..... pg. 1
GABA alterations in schizophrenia ..... pg. 2
Regions of interest in the current study ..... pg. 6
Hippocampal changes in schizophrenia ..... pg. 7
Rhesus monkey model ..... pg. 8
Predictions ..... pg. 9
Significance ..... pg. 9

Methods ..... pg. 10
Subjects and lesions ..... pg. 10
Brain harvesting ..... pg. 11
Designation of layers ..... pg. 12
Data analysis ..... pg. 13
Randomization of tissue sections ..... pg. 13
Cell count ..... pg. 14
Statistical analysis ..... pg. 15
Effect size ..... pg. 16
Layer area and Volume ..... pg. 16
Coefficient of Error ..... pg. 17

Results ..... pg. 18
Parvalbumin Analysis ..... pg. 18
Parvalbumin-immunoreactive neuron density ..... pg. 18
PV density effect size ..... pg. 19
Total parvalbumin cell estimate ..... pg. 20
Correlation between hippocampal lesion size and average PV cell density ..... pg. 21
Coefficient of error ..... pg. 22

Discussion ..... pg. 22
Overview ..... pg. 22
Possible mechanisms of GABA circuit alteration ..... pg. 23
Implications of parvalbumin circuitry alteration ..... pg. 25
Lateralized effects of hippocampal lesion ..... pg. 27
Limitations ..... pg. 29
Functional significance ..... pg. 30
Conclusions ..... pg. 32
Future directions ..... pg. 32

References ..... pg. 35
Figures ..... pg. 45
1: Macroscopic view of hippocampus and prefrontal cortex ..... pg. 46
2. Dorsal lateral prefrontal cortex ..... pg. 46
3. Photo reticle ..... pg. 47
4. Optical fractionator ..... pg. 47

5. Stereological setup ....pg. 48
6. Cortical layers ....pg. 49
7. Antigen retrieval ....pg. 49
8. Immunohistochemistry ....pg. 50
9. GABAergic circuitry ....pg. 51
10. Differential shrinkage ....pg. 51
11. GABAergic developmental trajectory ....pg. 52
12. Tissue series ....pg. 53
13. Parvalbumin-stained cells ....pg. 54
14. Somatostatin-stained cells ....pg. 54
15. PV-cell density by hemisphere ....pg. 56
16. PV-cell density by group ....pg. 56
17. Total PV-positive cell count by hemisphere ....pg. 57
18. Total PV-positive cell count by group ....pg. 58
19. Lesion percentage by PV count average ....pg. 59
20. Summary statistics ....pg. 60
21. Hemispheric volumes ....pg. 60
22. Coefficient of error ....pg. 60
23. Antigen retrieval manipulations ....pg. 62
24. PV-positive cell density calculations ....pg. 63
25. PV-positive cell estimation calculations ....pg. 63
26. Lesion percentage ....pg. 64
27. Volume reduction ....pg. 64
28. Monkey behavioral data ....pg. 65

Appendix ....pg. 62
CE equations ....pg. 66
Supplemental writings ....pg. 68
Other GABAergic Alterations in Schizophrenia ....pg. 69
GABA ....pg. 71
Histological Processing: GRα2 and Somatostatin ....pg. 72
Somatostatin Staining ....pg. 75
GABA Receptor Alpha Two Subunit Staining ....pg. 75
Coefficient of Error ....pg. 75
Stereology ....pg. 76

Introduction:

GABA is the primary inhibitory neurotransmitter in the human brain and is implicated in aspects of cognition including working memory and cognitive flexibility (Murray et al., 2015). Under normal conditions, working memory is associated with the dorsolateral prefrontal cortex (dlPFC). Prefrontal cortex (PFC) GABA plays a fundamental role in human behavior and a perturbation to GABAergic circuitry in the PFC may manifest as behavioral deficits, including problems with working memory (Murray et al., 2015). The conceptual approach for this project focused on the findings that humans with neurodevelopmental disorders, which may include schizophrenia and autism, suffer from deficits in working memory (Lewis and Hashimoto, 2007; Huang et al., 2014; Park and Gooding, 2014). In addition, work done by Heuer and Bachevalier (2011) showed that the monkeys used in this study displayed working memory deficits. We chose to assess the density of GABAergic neurons in the regions of interest because a large body of research has established normal developmental trajectories and has also reported changes in GABA levels in tissue from humans with schizophrenia. Thus, the ultimate goal of this project was to investigate the anatomical correlates of working memory and to determine to what degree, if any, alterations mirrored the reported behavioral deficits following a neonatal hippocampal lesion.

GABA and GABAergic neurons

γ-Aminobutyric acid, more commonly referred to as GABA, is the primary inhibitory neurotransmitter in the vertebrate brain. GABA is nearly ubiquitous in the brain, a part of almost all circuits, and interacts with at least twenty distinct receptor subtypes (Nutt, 2006; Kilb, 2012). While GABA receptors can be either metabotropic or ionotropic, the most common GABA receptors in the human brain are those described as ionotropic GABA-A receptors (Olsen and

DeLorey, 1999). GABA-A receptors are associated with chloride entering the cell and are believed to modulate the positive symptoms of schizophrenia, which include hallucinations and disorganized speech (Steeds, 2015; Olsen and DeLorey, 1999). On the other hand, $GABA_B$ receptors are metabotropic receptors associated with potassium entering the cell and are believed to play a role in the modulation of the negative symptoms of schizophrenia which include catatonia and apathy (Olsen and DeLorey, 1999; Kantrowitz, Citrome, and Javitt, 2009). Generally, prefrontal GABA is important for sustained reward-related signaling, whereby a deficit may result in the inability to make appropriate, context-specific decisions. (Bissonette and Roesch, 2015). Similarly, the GABAergic system is most likely involved in the valuative system which responds to rewards (Hayes, 2015). Firing of the GABA neuron produces an inhibitory postsynaptic potential (IPSP) in the postsynaptic cell, which for this project are frontal cortex pyramidal cells. Further, all GABA-A receptors are classified as heteropentamers, requiring the presence of at least one α subunit and one β subunit. The most common GABA-A receptor makeup in the human brain consists of two α's, two β's, and a single γ subunit (Olsen and DeLorey, 1999; Davies, 2003). Thus, not only is GABA circuitry highly integrated across the brain, it also plays a complex role in the prefrontal cortex, modulating aspects of behavior tied to schizophrenia.

GABA alterations in schizophrenia

As mentioned above, the conceptual approach of this project was based on the findings of GABAergic alterations characteristic of the neurodevelopmental disorder schizophrenia. First, a brief description of the schizophrenia is integral to an understanding of how our project was developed and is relevant to the current body of scientific literature. The current understanding

of schizophrenia etiology suggests that the disease develops in individuals with a genetic predisposition, triggered by certain environmental and life events, including major stressors (Selten, Cantor-Graae, and Kahn, 2007; Tessner, Mittal, and Walker, 2011). The stress-diathesis model is the psychological theory that the combination of environmental and genetic risk factors can result in a disorder (Lazarus, 1993). This idea applied to schizophrenia is known as the neurodevelopmental hypothesis of schizophrenia, and suggests that such stress events may take place during an individual's prenatal or postnatal development (Piper et al.,2012). Some of the primary environmental factors that are believed to play a role in schizophrenia include exposure to certain viral infections during neurodevelopment and pregnancy, malnutrition in utero, complications during birth, and later onset psychosocial factors including abnormal interpersonal relationships (NIMH, 2016). Onset appears to require an increased accumulation of stress events relative to healthy controls, and based on the timing of most diagnoses, a disrupted process of synaptic pruning and myelination likely play a role in symptom onset (Picchioni and Murray, 2007; Clemmensen, Vernal, and Steinhausen, 2012). While the disease etiology of schizophrenia is incredibly complex, it is a useful model for studying the GABAergic circuitry as well as the implications of GABA dysfunction.

Eugene Roberts discovered the presence of GABA as an inhibitory neurotransmitter in 1950, but was also the first to associate abnormal levels of GABA with the deficits characteristic of schizophrenia (Garbutt and van Kammen, 1983). According to Lewis and Hashimoto (2007), GABA plays an important role in coordinating and sustaining the firing of pyramidal neurons in the dlPFC during working memory tasks which are negatively impacted as part of schizophrenia. Further, older studies suggest there is an abnormal disruption of GABAergic signaling in patients with schizophrenia, including perturbation of the normal synthesis, reuptake, and receptor

activation of GABA. In 1991, Squires and Saederup proposed that schizophrenia is the result of hyperactive GABA receptors, and additional research linked schizophrenia to reduced GABAergic inhibition on AMPA/kainate glutamate receptors as well as loss of NMDA receptor-bearing GABAergic neurons (Deutsch, Rose, Schwartz, and Mastropaolo, 2001; Olney and Farber, 1995). Such hypo-functioning within the GABAergic system may result in an overactive striatal dopamine system which could in turn result in some of the symptoms associated with schizophrenia (Breier et al., 1997).

As recently as twenty years ago scientists found a significant reduction of GABA in Brodmann Areas 9 and 10 of the prefrontal cortex in schizophrenia patients (Perry, Geyer, and Braff, 1989). The GABA theory of schizophrenia is an explanation for the inherited GABA dysfunction characteristic of schizophrenia. The theory suggests that under normal circumstances, GABA interneurons receive NMDA-mediated glutamatergic inputs about the level of excitation in nearby cells. In schizophrenia, the input from NMDA receptors is in some way disrupted, reducing the level of feedback by GABAergic interneurons onto the nearby excitatory neurons (Gordon, 2010, Nakazawa et al. 2012). This model also explains why previous models, namely the dopamine theory of schizophrenia, would have implicated excitatory neurotransmitters in the brain. While drugs that increase dopamine activity in the brain, namely amphetamine and cocaine, can result in psychosis-like behavior, some treatments to reduce psychosis work nearly immediately at the physiological level, but may take weeks to demonstrate any appreciable symptom relief (Weinberger, 1987 and Thompson, Pogue-Geile, and Grae, 2004).

In addition, a large amount of research has established that the number of PV-immunoreactive cells, both the chandelier and basket subtypes, is significantly reduced in

postmortem cortical tissue of humans with schizophrenia (Beasley et al. 2002; Gill and Grace 2014; Lewis and Hashimoto 2007). Previous research established this result, but found that the loss was specific for layers III and IV within Brodmann Areas 9 and 46 (Beasley and Reynolds, 1997). In layer III, the superficial third of the layer (called layer IIIA) shows a more pronounced loss of PV-containing neurons than the deep two-thirds of the layer (called layer IIIB) (Lewis and Hashimoto 2008).

Work by Cruz et al. (2003) demonstrated the developmental trajectories of parvalbumin and the GABA receptor alpha 2 subunit (GRα2) in the prefrontal cortex of rhesus macaque monkeys. The research showed that the number of parvalbumin cells increased within the PFC until pruning onset at approximately one year of age. In contrast, GRα2 subunit-positive axon initial segments peaked at birth and underwent a dramatic downregulation. The same work showed that at age 7, following development, parvalbumin was found at the highest levels in cortical layer III while GRα2 subunits were predominantly in cortical layer II of the rhesus monkeys (Cruz et al., 2003). The relative isolation of parvalbumin and GRα2 to specific layers and their specific developmental trajectories made them attractive targets for our analysis. While many neuron types are associated with the extremely complex GABAergic circuitry in the human and rhesus monkey brain, the three that this research was concerned with were Parvalbumin (PV), GABA Receptor Alpha Two Subunit (GRα2), and Somatostatin (SST). Due to its nearly ubiquitous presence and fundamental role in the frontal cortex, any alteration to the GABAergic circuitry may underlie neurodevelopmental disorders that are characterized by deficits in the processing associated with this brain region (Kilb, 2012)

Regions of interest in the current study

While schizophrenia and other neurodevelopmental disorders may impact numerous regions in the human brain, the current research study focused on specific areas of the brain that are believed to play a major role in the etiology of schizophrenia. The major regions involved are the hippocampus, a region of the brain that develops early in life and is connected to the prefrontal cortex, and the dorsolateral prefrontal cortex (dlPFC), also known as Brodmann area 46d (Petrides and Pandya, 1999).

The hippocampus is a limbic system structure located within the medial temporal lobe. Under normal working circumstances, the hippocampus is primarily implicated in memory consolidation, the process of moving memories into the cortices for long term memory, as well as spatial memory. Because of its relatively early development, the hippocampus is believed to play an important role in the development of other regions of the brain, particularly the prefrontal cortex, which undergoes a far more protracted development in both humans and nonhuman primates (Bourgeois and de Villers-Sedani, 1994; Payne, Machado, Bliwise, and Bachevalier, 2010).

In terms of the current research study, there are two well-defined regions of the prefrontal cortex that are believed to be connected in some capacity to the hippocampus. First, there is an indirect, multisynaptic pathway between the dorsolateral prefrontal cortex (dlPFC), primarily BA 46d, and the hippocampus (Hirata et al., 2013; Chlan-Fourney, submitted). In addition, there exists a more direct, monosynaptic pathway from the ventral CA1 region of the hippocampus and subiculum to the ventromedial prefrontal cortex (vmPFC) (Barbas and Blatt, 1995). Under normal working conditions, the dlPFC is strongly implicated in monitoring processes as part of episodic and working memory (Blue, Kazama, and Bachevalier, 2013) while the vmPFC is

implicated in emotional decision making (Bechara, Tranel, and Damasio, 2000). Therefore, disruption to these regions, by way of a neonatal lesion to the hippocampus before the complete development of the frontal lobe, may result in abnormal organization within the prefrontal cortex, similar to that seen in the brains of humans with schizophrenia. Such a disruption may manifest behaviorally as impairment of working and episodic memory processing. Ultimately, such perturbation to the system could provide a useful model for understanding the role of prefrontal inhibitory circuitry in the development of schizophrenia.

Hippocampal changes in schizophrenia

While they may not be always be the result of a neonatal lesion, structural hippocampal differences seem to play some role in schizophrenia. Whether these differences cause certain symptoms of schizophrenia or whether they are a result of the factors that cause schizophrenia is not entirely defined. For example, several studies have demonstrated that the volume of the hippocampus is reduced in the brains of patients with schizophrenia by an average of 5% (Lawrie and Abukmeil, 1998; Nelson, Saykin, Flashman, and, Riordan, 1998). Furthermore, Lewine (1995) found a significantly greater number of morphological anomalies in the brains of both patients with schizophrenia and schizoaffective disorder as compared to healthy controls, suggesting the normal development of those affected with the disorder was in some way altered. Importantly, the size of the hippocampus at the time of first symptom is not the end of hippocampal reduction. In a longitudinal study performed on patients diagnosed with schizophrenia, the volume of the hippocampus, within the left hemisphere specifically, was significantly reduced as compared to volume at first symptom (Rizos et al., 2014). Further, Kawano et al. (2015) found that patients with chronic schizophrenia had the greatest reduction within the left hippocampus on average even when corrected for age, sex, and total brain volume.

Even more, an additional analysis of a subset of both the first episode patients and controls taken was conducted six months after the original study. The patients with schizophrenia experienced an additional reduction in left hemisphere hippocampus relative to the first assessment (Kawano et al, 2015).

Rhesus monkey model

The rhesus monkey, or *Macaca mulatta*, is a long-established and valuable model for neuroscience research, both basic and translational. Rhesus monkeys are Old World Monkeys, a taxon to which humans also belong. Rhesus monkeys are widely available, but native to South, Central and Southeast Asia, and occupy a variety of habitats including areas with and without tree cover (Timmins, Richardson, Chhangani, and Yongcheng, 2008). In addition, modern-day rhesus monkeys are often found living in close proximity to humans and even use resources allotted by an urban environment to create larger troops than can be supported in the natural habitats (Rishi, Sinha, and Radhakrishna. 2013). Because rhesus monkeys are relatively more manageable in captivity as compared to chimpanzees, they are a favorite among researchers using a nonhuman primate model. That said, the rhesus monkey model is quite expensive in relation to other mammals, and thus, it is important to base all nonhuman primate research on prior studies using lower order models. For example, research using rodents, including rats, suggested that a neonatal lesion to the ventral hippocampus yields animals with working memory and spatial memory deficits, similar to the cognitive symptoms of schizophrenia described above and similar to the nonhuman primate model in this project (O'Donnel, 2012).

In 2007, the rhesus monkey became the second nonhuman primate to have its genome sequenced, yielding a 93% similarity to humans (Zahn, Jasny, Culotta, and Pennisi, 2007). Similarly, the brains of rhesus monkeys and humans have high anatomical and functional

similarity which allows for extrapolation of research findings in monkeys to humans (Nakahara, Adachi, Osada, and Miyashita, 2007; Payne, Machado, Bliwise, and Bachevalier, 2010). Of additional importance, the monkey model allows researchers to conduct more invasive techniques, as compared to research that can be ethically conducted in humans. Specific to this project, the rhesus monkey model allowed us to perform longitudinal studies on lesion models as well as tightly control all environmental variables to which the monkeys are exposed (Passingham, 2009).

Predictions

As part of this investigation, we selected markers of the GABAergic system that are altered in human schizophrenia patients and for which we were able to generate clear predictions and quantification strategies for assessment. Our previous research, conducted over summer 2015, sought to characterize the distribution of parvalbumin, calbindin, and GABA Receptor α2 (GRα2) within the dlPFC. The primary target of this honors project is the PV neuromarker. Further, over the course of our summer, fall and early spring semester work, we were unable to immunohistochemically visualize GRα2 and SST. While staining of calbindin was achieved, we felt that PV was more important given the shift in focus of recent schizophrenia research.

Based on the large body of literature showing that parvalbumin-containing neurons are reduced within the dlPFC of schizophrenia patients, we predicted that there would be a decreased number of PV cells in the lesioned monkeys as compared to controls.

Significance

This study was completed in order to better understand how neonatal hippocampal lesions impact PV-immunoreactive dlPFC circuitry as it relates to deficits characteristic of

human neurodevelopmental disorders. There is currently a large body of research relating to alterations in GABAergic circuitry within human models of schizophrenia. It was this body of research that ultimately informed the specific neuromarkers that were analyzed as a part of this process.

Further, our data will ultimately be compared to behavioral data generated by Heuer and Bachevalier (2011). While behavioral data from both lesioned monkeys and humans with schizophrenia have been published, there is no work to our knowledge that has investigated the circuit-level impact of hippocampal lesion in models of early insult pathogenesis of schizophrenia. This analysis will help build a more comprehensive understanding of the interaction between the hippocampus and dlPFC as it relates to symptoms of schizophrenia.

Methods

Subjects and lesions

A total of eight rhesus monkeys (*Macaca mulatta*) were analyzed as a part of this project. At 10-15 days postnatal, four monkeys received bilateral hippocampal lesions of variable size and four were sham-operated controls, meaning they underwent a surgical procedure at the same time as the experimental animals, but did not receive hippocampal lesions. Both male and female monkeys were included in each group. The lesions were carried out by Dr. Jocelyne Bachevalier using ibotenic acid, a neurotoxin that selectively destroys cells bodies, and precautions were taken to minimize the amount of neurotoxin exposed to other parts of the brain. Details of the surgical procedure are outlined in previous publications including Goursaud and Bachevalier (2007). All animal work performed by the Bachevalier Lab as part of this project, including the administration of neonatal hippocampal lesions and recording of analyzable behavioral data, followed an IACUC relating to a grant received by Dr. J. Bachevalier from the NIH.

Further, using images obtained from fluid attenuated inversion recovery (FLAIR) MRI, the Bachevalier Lab calculated the percentage of volume reduction within each hippocampus as well as the average reduction within a given monkey and the weighted average of reduction (see Appendix; Heuer and Bachevalier, 2011). Ultimately the Bachevalier Lab will analyze prepared Nissl (thionin) and Gallyas stained sections to confirm the extent of the individual hippocampal lesions.

Brain harvesting

After all behavioral studies were concluded, both the lesioned and the non-lesioned monkeys were euthanized and tissue was harvested by the Bachevalier Lab according to procedures described in their previous study (Goursaud and Bachevalier, 2007). Prior to extraction, brains were perfused with a 0.9% saline solution and then fixed with a 4% paraformaldehyde (PFA) solution. The combination of these procedures clears blood from the brain and prevents the deterioration of the tissue before it can be analyzed. Following extraction, each brain underwent a series of cryoprotection treatments whereby they were immersed in increasingly concentrated solutions of sucrose, up to 30%, and sodium azide. Cryoprotection prevents brain tissue from forming ice crystals which can disrupt the normal tissue sectioning process using a freezing microtome. Several 1-in-10 series of 50 micron (μm) sections were prepared for this project. A series of reference sections was prepared via cresyl and myelin staining by the Bachevalier Lab in order to confirm cortical layers. A similar series was prepared in order to analyze PV-immunoreactive tissue across the entire region of interest. Additional tissue was used in other projects or stored in a cryoprotectant solution at low temperature in anticipation of use for additional analyses.

Histological Processing: Parvalbumin

All immunohistochemistry work followed a general standard in our lab that is consistent with other work in the field (Rodman et al., 2001; Lavenex, Lavenex, Bennett and Amaral, 2009). Prior to the immunohistochemistry procedure, sections were washed in four rinses for thirty minutes each in 0.1M phosphate buffer (PB) to remove residue from storage solution. After the wash, sections were incubated overnight in a refrigerated solution containing PB with 0.3% Triton, 5% normal horse serum as the blocking agent, and a primary antibody (anti-mouse) directed against parvalbumin at a dilution of 1:10,000 (Swant, Bellinzona, Switzerland). The use of this concentration followed a dilution series that yield staining of cell bodies and processes as well as a pattern of staining in the cortex consistent with our expectations. The antibody was evaluated for specificity and potency by Swant using indirect immunofluorescent labeling, immunoenzymatic labeling, and by radioassay. Specificity was also confirmed by additional published literature (Celio and Heizmann, 1981; Schwaller et al., 1999). Following a set of three ten-minute rinses, the PV antibody reaction was localized by incubation for one hour at room temperature in a solution of phosphate buffer with 0.3% Triton and a secondary antibody, anti-mouse biotinylated immunoglobulin G (BIgG), at a dilution of 1:200. After an additional set of rinses, the avidin-biotin method, at a dilution of 1:100 with 0.3% Triton and salt, was used as a means of signal amplification. The final step of the IHC procedure used Diaminobenzidine (DAB) as the chromogen. The sections were incubated in 0.025% DAB for 10 minutes then exposed to 0.01% hydrogen peroxide for 1 minute and 30 seconds, which catalyzes the oxidation of DAB to its colored form.

Following the immunohistochemistry procedures, the stained sections were thoroughly rinsed in PB and mounted on subbed, glass slides. The slides were then dehydrated in a mix of

chloroform and alcohol before being counterstained with Giemsa (Iniguez et al., 1985). Last, sections were cover-slipped with Permount.

Designation of Layers

For this project, we operationalized the middle 1/3 portion of the upper bank of the principal sulcus, BA 46d, as the region of interest (Saleem and Logothetis, 2006; see Figure 11). First, we created a virtual tracing of each hemisphere such that those counting could blindly find the region of interest using the MD Plot software and Minnesota Datametrics hardware. We operationalized and traced layers based on previous work (Petrides and Pandya, 1999; Preuss and Goldman-Rakic, 1991). Because tissue stained for PV was also counterstained with Giemsa, which stains all cell bodies, layers could be determined with relative ease. The tracings, within the upper bank of the principal sulcus included all six cortical layers with Layer IIIA and Layer IIIB demarcated (see Figure 6). For the purposes of this project, we traced Layer IIIA as the upper one-third of cortical Layer III while the bottom two-thirds constituted Layer IIIB (Petrides and Pandya, 1999; Peters, Leahu, Moss, and McNally, 1994; Preuss and Goldman-Rakic, 1991; Sesack, 1998 and Chlan-Fourney, submitted). As was often possible, we used the thin, cell-sparse interlaminar region, to determine the boundary between the smaller pyramidal cells of Layer IIIA and the larger pyramidal-shaped neurons of Layer IIIB.

Data Analysis

Randomization of tissue sections

All tissue was analyzed blind such that I assigned each monkey a random case number and each section a random number using www.Random.org. Dr. Rodman then re-randomized the cases and sections so that neither of us knew the identity of a given case or section. In all

instances, both hemispheres of a given section were assigned the same randomized number and analyzed at the same time.

Cell count

For the actual counts of this project, we used a photo-reticle in the right-hand eyepiece of the Optiphot-2 microscope, with a superimposed framing screen on the image, like those seen in cameras. The photo reticle allowed us to frame virtual exclusion and inclusion lines, such that if half or more of a given cell fell within the inclusion line it was counted, and if a cell fell on the exclusion line it was excluded (Altunkaynak, 2012; see Figure 3). In order to count cells in three dimensions we incorporated the optical disector principle of stereology. We established a so-called reference section at a terminal depth of the tissue where no cells were in focus. Then, using the microscope's fine focus, we moved through the tissue to a point where the first cell was in the plane of focus. At this point, known as the lookup section, we only counted those cells that were focused in the plane of the section (Disector; Kaplan, 2012). Neurons were counted if they were stained completely throughout the cell body, and if a neuronal process could be identified. Stained structures that did not meet the above criteria were rejected. Furthermore, our stereological method incorporated the use of an optical fractionator technique, another key stereological technique, which employed a sampling grid of 150 μm x 150 μm and a counting frame of 70 μm x 70 μm. A transparency with the sampling grid was laid over the computer screen such that the rows were oriented at a random latitude that did not match the tracing of Layer IIIA on the screen such that counts were started at a random point within the tissue (see Figure 5). All the counting frames that fell at least 50% within the portion of Layer IIIA falling within the virtual middle ⅓ of the upper bank of the principal sulcus were used for counting.

Approximately twenty to thirty counting frames met this criterion within each hemisphere per section.

Within each of the eight monkeys analyzed in this study, we counted at an average of 6-8 sections through the dlPFC for a total of 116 counts, 61 in Neo-H monkeys and 55 in Neo-C monkeys. Consistent with general stereology guidelines, we made approximately 20-25 separate counts per section in order to bring the coefficient of error in sampling variance to less than 0.05 (Scheaffer, 1996). Ultimately, we counted a total of 2681 cells as part of this study.

Both Dr. Rodman and A. Howley conducted a comparable number of counts in each brain in addition to my own counts. To start the counting process, all three counters worked together to develop and master the criteria for counting an individual structure as a cell. In addition,we each counted some of the same counting frames and compared results to decrease variability among counters and increase the inter-rater reliability across all the counts.

Statistical Analysis

As a part of this study we analyzed several relationships between the two groups. First, we performed several comparisons of the means between different groups. These groups included Neo-H versus Neo-C, the left hemisphere between Neo-H and Neo-C, and the right hemisphere between Neo-H and Neo-C. Assumptions of normality were confirmed for the analyses of the PV cell density by group and PV cell density in the left hemisphere of Neo-H versus Neo-C and thus a two-sample t-test was performed each. Because the analysis of the PV cell density of the right hemisphere between Neo-H and Neo-C was not normally distributed, we used a nonparametric, Mann-Whitney U Test. Further, in order to understand the degree to which the hippocampus impacts the development of the dlPFC, a correlation analysis between the size of each hippocampal lesion and PV cell density was important. Using Microsoft Excel, we

performed a regression analysis to determine the coefficient of determination, a measure of how well the data follow the line of best fit.

Effect size

In addition to a t-test and Mann-Whitney U test, we performed an analysis of the effect size for calculations of PV density. The effect size, which is often used as a supplement to the traditional p-value, is a measure of the magnitude of the difference between groups (Olejnik and Algina, 2003; Sullivan and Feinn, 2012). Further, the effect size may be considered "substantive" while the p-value is "statistical" in that the p-value can only indicate that an effect is present while an effect size informs of the effect's magnitude (Sullivan and Feinn, 2012). The formula for the calculation of effect size differs between populations that are normally distributed and those that are not. Because one of our populations, the right hemisphere of the Neo-C cases, did not pass the normality test, we did not use the standard "Cohen's d" formula but instead the formula $r = Z/\sqrt{N}$where Z is the Z-score and N is the total number of samples (Becker; 2000; Olejnik and Algina, 2003; Sullivan and Feinn, 2012; Effect Size). This calculation produces scaled values such that an effect size of $r = 0.1$ is considered small, 0.3 is considered medium, 0.5 is considered large (Sullivan and Feinn, 2012).

Layer area and volume

In addition to a measure of mean PV-immunoreactive neuron density, we also performed estimations of total cells in order to extrapolate our stereological counts to the entirety of our region of interest across a given hemisphere. This measurement required we know the volume of the ROI, specified as the portion of Layer IIIA falling within the virtual middle ⅓ of the upper bank of the principal sulcus (see Figure 2; 11). In order to find this volume measurement without

a stereological microscope, we used images of each hemisphere traced virtually by Dr. Rodman for the stereological counting. Each image was uploaded onto the imaging software Canvas (Deneba Systems, Inc.) which allowed us to trace the relevant portion of Layer IIIA and provided us with a precise area and perimeter measurement for each outline. Area values were then used with the standard tissue thickness, 50µm, in order to calculate the volume of each section using the end-area formula (½ D (A_1+A_2). The volumes of each section were then summed to find the total hemispheric volume for the ROI using the Cavalieri Estimator. In order to get a multiplication factor, the calculated hemispheric volume was divided by the volume of the counting frame, a constant 0.000245mm^3, based on the 70µm x 70µm counting frame. This value was multiplied by the average cell density for the specific hemisphere in question and then by the number of sections containing the region of interest, yielding an estimation of the total number of cells within the region of interest. Estimates were qualitatively compared between Neo-H and Neo-C groups as well as between hemispheres in the two groups.

Coefficient of error

In addition, both the area and perimeter measurements derived from the Canvas software were used in the analysis of the coefficient of error. The CE expresses the adequacy of the sampling based on the intrinsic variability of both the tissue and the distribution of the particles being measured. Further, the equation adapts to the contour of sections based on the numbers fed into the equation such that data must be properly ordered (Altunkaynak, 2012; Stereo Investigator 8.0; see Appendix). In other words, the variance of a count can be estimated. Additionally, we replicated previous stereological counting strategies by regarding Layer IIIA across hemispheres as individual structures, as done in examples presented in Altunkaynak

(2012). Thus, we were able to calculate a CE in individual hemispheres, brains, and across the entire study.

Results

Parvalbumin analysis

The primary GABA marker studied as part of this project was parvalbumin. The PV staining worked well allowing us to visualize morphology and shape of the labeled cells. Generally, the cell bodies were stained through their full extent making them easily distinguishable from non-specific background staining as was part of our counting criterion. Finally, dendritic processes of immunoreactive neurons were strongly labeled and visible, and the overall laminar pattern was similar to those reported in the literature (Cruz et al., 2003). Following immunohistochemistry and stereology procedures, we analyzed both the average PV cell density within our counting frames as well as estimates of total cells within the volume of the ROI in the upper bank of the principal sulcus (see Figure 11).

Parvalbumin-immunoreactive neuron density

After the addition of two monkeys and four hemispheres to our original analysis of PV cell density, this project analyzed a total of eight monkeys and sixteen hemispheres. We performed both a statistical analyses between experimental groups (lesioned and non-lesioned monkeys) as well as across hemispheres.

For our PV cell density by group, Neo-C versus Neo-H, mean PV cell density within Neo-H experimental group ranged from 0.320 to 1.75 neurons per counting frame with an average of 1.07 ± 0.295 (SE=0.0377). The average PV-immunoreactive cell density within the control group ranged from 0.400 to 1.77 neurons with an average of 0.943 ± 0.269 (SE=0.0347).

The two-tailed P value between the Neo-C and Neo-H groups was 0.018, t(119) = 2.41 (Figure 15).

Further analysis was conducted within individual hemispheres between the experimental and control hemispheres. First, the analysis of the left hemisphere of Neo-H monkeys yielded an average PV cell density ranging from 0.405 to 1.75 neurons per counting frame with an average mean of 1.10 ± 0.319 (SE = 0.058). A similar analysis of the left hemisphere among the Neo-C monkeys yielded an average PV cell density ranging from 0.5 to 1.36 with an average mean of 0.872 ± 0.222 (SE = 0.041). The two-tailed P value between the Neo-C and the Neo-H groups was 0.0018 with t(58) = 3.28 (Figure 14).

Finally, an analysis was conducted between the right hemispheres of both the Neo-H and Neo-C monkeys. The right hemisphere of the Neo-H monkeys had a mean PV cell density ranging from 0.32 to 1.48 neurons per counting frame with an average mean of 1.03 ± 0.269 (SE = 0.048). The right hemisphere of the Neo-C monkeys had an average PV cell density ranging from 0.4 to 1.77 with an average mean of 1.00 ± .300 (SE= 0.055). The Mann-Whitney U test yielded a two-tailed p-value of 0.681 (U' = 494) (Figure 14).

PV density effect size

In addition to p-values, we calculated the effect size for each group analyzed for PV-immunoreactive cell density in order to determine the magnitude of the effect. The effect size for the comparison of the left hemispheres of Neo-C monkeys and Neo-H monkeys was 0.847 which can be described as a large effect magnitude and suggests that the two groups were quite different (Sullivan and Feinn, 2012). The effect size of the right hemispheres between Neo-C and Neo-H monkeys was 0.098 which is a small effect magnitude and suggests that the two populations did not vary, consistent with our analysis above. Finally, the effect size of the overall

comparison between Neo-C and Neo-H PV cell density was 0.437 which can be considered a medium effect size. In each case, the effect size provided a similar result to the corresponding p-value calculated above.

Total parvalbumin cell estimate

In addition to measurements of PV cell density, we estimated the total number of PV cells within our region of interest in the bank of the principal sulcus. In order to do so, we calculated the volume of the region of interest and used that with the average PV cell density per counting frame to extrapolate our counts across the entire layer IIIA of area 46d. We found that the total PV cell count estimations were higher in the Neo-H monkeys as compared to Neo-C monkeys. Further, we found that the highest number of cells was in the left hemisphere of the Neo-H group, but the estimated number within the right hemisphere of the Neo-H monkeys was also larger than that in the right hemisphere of Neo-C monkeys. The total average PV-immunoreactive neuron estimation throughout the ROI in the Neo-C group was 343,419 cells while the Neo-H average was 416,668 cells (Figure 24). The average left hemisphere estimation for Neo-C was 175,971 PV-reactive neurons while the average for Neo-H left hemisphere was 227,254 neurons. Finally, the average right hemisphere estimation for Neo-C was 167,448 PV-reactive neurons in comparison to an average of 189,414 neurons in the Neo-H group. All groups, Neo-C, Neo-H and their subdivision based on hemisphere, had a sample size of four for the total cell estimates in the ROI and thus were not compared statistically. These results are consistent with PV densities that showed an increase in PV cell density within the Neo-H monkeys.

Correlations between hippocampal lesion size and average PV-positive cell density

Even when great care is taken to create similar surgical environments, including the injection of similar amounts of ibotenic acid at multiple sites within the hippocampus, there is no way to guarantee lesions of identical size among brains or even across hemispheres of the same brain (Heuer and Bachevalier, 2011). Understandably, the monkeys within this study had lesion sizes of varying degree, even across hemispheres in the same monkey. That said, variable lesion size can be used to compare the extent of the volume reduction to PV cell density, a description of which can be found in the Results section. Because four monkeys were bilaterally lesioned and analyzed as a part of this study, there were a total of eight lesioned hemispheres. The range of those lesions as assessed by FLAIR range from 10.6% - 72.8% of total hippocampal volume reduction (Heuer and Bachevalier, 2011; Figure 27). Further, all monkeys sustained asymmetrical lesions such that left and right hemisphere lesions ranged from 10% - 28% total volume reduction. If the hippocampus does play a role in the development of the dlPFC, the degree to which the hippocampus is damaged should correlate with counts in the dlPFC.

Casual inspection of the data suggested that the size of a given hippocampal lesion was related positively to the average density count within the dlPFC of the same hemisphere such that an increase in lesion percentage resulted in an increase in PV density. The degree to which the lesions were asymmetrical within a given brain did not appear to impact the relative densities of the two hemispheres. For instance, in monkey E3, which had the most asymmetrical hippocampal lesions, differing by nearly 50%, the two hemispheres differed in counted PV density by only five percent. A scatter plot analysis of the relationship between lesion size and cell count density within the eight lesioned hemispheres by regression analysis yielded a coefficient of determination (R^2) value of 0.710. A similar analysis including only the lesion

percentages and PV cell density counts of the left hemisphere yielded an R^2 value of 0.878. The correlation across only the right hemisphere lesions yielded an R^2 of .838.

Coefficient of Error

The average CE for the entire study was 0.031 which falls below the standard 0.05 threshold (StereoInvestigator 8.0). The maximum and minimum CE determined within individual hemispheres were 0.016 and 0.041 respectively, suggesting that counting was sufficient in all hemispheres (Figure 22).

Discussion

Overview

In order to assess disruption of dlPFC development following neonatal hippocampal lesion, we analyzed the density of parvalbumin-positive cells in Layer IIIA of BA 46d. PV cell density in this ROI of Neo-H and Neo-C monkeys showed a significant increase in the number of parvalbumin cells within the lesioned monkeys as compared to the control cases contrary to our prediction based on work reporting decreases in PV-immunoreactive cell numbers from tissue of humans with schizophrenia (Beasley et al. 2002; Gill and Grace 2014; Lewis and Hashimoto 2007). While disruption of the normal PV circuitry may be a major factor in development of schizophrenia, neurodevelopmental disorders are extremely complex and likely result from the accumulation of many factors, including genetic predisposition and environmental stressors beyond the lesion explored in this project (Selten, Cantor-Graae, and Kahn, 2007; Tessner, Mittal, and Walker, 2011; Piper, 2012; NIMH, 2016).

In addition, comparisons of PV cell density between the left hemisphere of Neo-H and Neo-C also showed a greater PV cell density within the lesioned cases, while right hemisphere

PV cell density was not significantly different when compared across the Neo-H and Neo-C groups. These results suggest differential development between the right and left hemisphere in terms of the prefrontal cortex.

Because the number of neurons in the adult rhesus macaque PFC and hippocampus remains largely preserved during normal development (O'Donnell, Rapp, and Hof, 1999; Merrill, 2000; Keuker, Luiten, and Fuchs, 2003) any shift in the total number of PFC neurons may be representative of a dysfunctional developmental trajectory. As discussed in the Introduction, and elaborated on below, PFC GABA circuitry is highly complex and integral to many aspects of normal functioning. Such perturbed circuitry may impact an individual's ability to perform specific tasks, including working memory. Beyond an analysis of our results, I will discuss possible implications, mechanisms, limitations, functional significance and the future goals important to understanding the development of GABAergic circuitry in the PFC.

Possible mechanisms of GABA circuit alteration

An understanding of the systems-level circuit linking the hippocampus to the dlPFC is useful in describing the impact of the hippocampus on dlPFC development. The hippocampus is connected to the dlPFC through several distinct pathways. For instance, in rhesus monkeys there is a multisynaptic circuit from the hippocampus through the nucleus accumbens, ventral pallidum, and ventral tegmental area to the dlPFC (Lodge and Grace, 2007). There also exists a smaller connection from the hippocampus to the dlPFC through the subiculum (Barbas and Blatt, 1995) as well as a connection from the hippocampus to the dlPFC through the vmPFC (Fan et al, 2013). In each case, the connections between the hippocampus and the dlPFC may be hemispherically unilateral or bilaterally identical in the rhesus monkey brain. That said, the hippocampus to cortex connections are generally ipsilateral such that circuits have not been

shown to cross from the hippocampus of one hemisphere to the prefrontal cortex of the other hemisphere (Aggleton, Wright, Rosene, and Saunders, 2015). Thus, early-life lesion of the hippocampus may perturb dlPFC development through several anatomical routes.

Work from the Bachevalier lab in our study's monkeys linked such a lesion of the hippocampus to a disruption in the functional connectivity of the dlPFC in neonatal hippocampal lesioned monkeys (Neo-H)(Meng, submitted). Using resting state functional MRI and DTI, a reduction of connectivity was found between the dlPFC and the regions mPFC, IT, MST, FST, PPC, and V4 (Meng, submitted). These results suggest that early lesion to the hippocampus has a profound impact on the functional connectivity of the dlPFC.

The normal developmental trajectory of the Rhesus monkey hippocampus involves a major period of maturation, mirrored by a shift in function, during the first two years (Payne, Machado, Bliwise, and Bachevalier, 2010). Interestingly, Reynolds and Beasley (2001), using human post-mortem tissue, found that parvalbumin immunoreactivity is not present in the dlPFC until relatively late in development, following the formation of synaptic contacts at 3-6 months of age. This finding highlights that the PV circuitry undergoes a significant window of vulnerability during neurodevelopment (Cruz et al., 2003). A hippocampal lesion during this vulnerable period likely impacts typical maturation of frontal cortex and its ability to function correctly. Our monkeys, lesioned between 10-15 days postnatal, are an adequate model of disruption prior to the normal development of PV circuitry since the rhesus monkey PV system appears to develop for several years, well beyond the postnatal period (Cruz et al., 2003; Figure 11). An increase in PV cells in the dlPFC specifically may have dramatic repercussions. Subsets of PV cells synapse onto the so-called axon initial segments of pyramidal cells, which have an important role in frontal lobe function because of their unique role in cell firing, allowing

contacts there to exert a relatively strong influence on pyramidal cell output (Sesack, 1995, 1998). The current findings are further evidence supporting the notion that hippocampal reduction as part of schizophrenia may alter the development of the PFC and manifest behaviorally.

Implications of parvalbumin circuitry alteration

The calcium-binding protein parvalbumin is implicated in regulation of vesicular release, second messenger production, synchronization of gamma oscillations and cognitive flexibility (Gonzalez-Burgos and Lewis, 2012; Auger and Floresco, 2015; Murray et al., 2015). Further, PV-positive cells are the largest class of GABAergic interneurons within the neocortex, and can be divided into two distinct subtypes: basket cells, also known as wide arbor cells, and chandelier cells. Basket cells primarily function as part of an inhibitory process while chandelier cells may carry out both inhibitory and excitatory functions. The basket type PV cells synapse primarily on the peri-somatic region of pyramidal neurons which are primarily located in the deep portion of cortical layer 3 as well as layer 4 in humans (Kawaguchi and Kubota, 1997). Chandelier neurons form synapses exclusively and densely onto the axon initial segments (AIS) of pyramidal cells and only contain the enzyme GAD67 (Gonchar, Turney, Price, and Burkhalter, 2002). Further, chandelier neurons receive synaptic input from mesocortical dopamine and thalamocortical glutamatergic projections, linking the GABA system to the dopamine system (Sesack, 1995, 1998).

Moreover, evidence from both rodent models and humans with schizophrenia suggest PV cells specifically play a key role in supporting working memory processing. Specifically, the selective inactivation of PV interneurons in the PFC equivalent of mice, using a DREADD

approach, results in deficits confined to cognitive processing including a significant increase in working memory errors. The same study found that selective disruption of SST in mice did not similarly impair performance on the working memory task (Murray et al., 2015). In addition, administration of the GABA-A receptor antagonist bicuculline to the rat PFC resulted in markedly increased errors and response latency on a spatial working memory task (Auger and Floresco, 2015). Thus, both specific and general PFC GABA inactivation results in working memory impairment.

Furthermore, a significant body of literature has shown that the PV class of GABA neurons plays a critical role in maintaining the brain's gamma oscillations. For instance, so-called synchronous gamma-oscillations are likely responsible for the normal working memory processing while asynchronous oscillations may underlie the cognitive symptoms, for example working memory deficits, seen in schizophrenia and other neurodevelopmental disorders (Gonzalez-Burgos and Lewis, 2012). Thus, any disruption to PV-positive cells, as demonstrated by our results, may alter gamma-oscillations and in turn manifest as deficits in working memory.

In addition to impaired working memory and gamma oscillations, parvalbumin dysfunction has been linked to the emergence of other maladaptive behavioral responses including an increased susceptibility to stress. For instance, the selective suppression of PFC PV interneurons in mice results in greater helplessness when exposed to an uncontrollable stressor as measured by escape latency and number of failed escape attempts (Perova, 2015). Furthermore, Piantadosi and Floresco (2014) found that administration of bicuculline to selectively disrupt prefrontal GABA more generally eliminated the ability of mice to form aversive memories, a potential proxy for the deficit in emotional regulation seen in schizophrenia. In primates,

injection of bicuculline in the dlPFC has been shown to increase the variability across in saccade response time to visual fixation on a target as compared to controls (Pouget, Wattiez, Rivaud-Péchoux, and Gaymard, 2009). These results indicate the role of prefrontal GABA in attention, with potential implications for better understanding and treatment of neuropsychological disorders including ADHD. Thus, prefrontal GABAergic circuitry appears to play a fundamental role in working memory and cognitive flexibility potentially through its role in maintaining gamma-oscillations. Disruption to GABAergic circuitry, in our project measured by alterations in PV-immunoreactive neurons, may underlie cognitive symptoms characteristic of neurodevelopmental disorders including schizophrenia.

Lateralized effects of hippocampal lesion

Beyond an analysis of PV-positive cell density, a correlation analysis of Neo-C and Neo-H groups separately showed that both left and right hemisphere hippocampal lesions were strongly correlated with PV-immunoreactive cell density. This suggests that monkeys with a more reduced hippocampus have higher PV density overall. (Figure 19). While both hemispheres independently have a high correlation between hippocampal lesion percentage and density of PV cells, our density results suggest a strong lateralization, such that the left hemisphere has a significantly greater number of total cells and density of PV-positive cells per counting frame. Our results suggest that the hemispheric effects of hippocampal lesion on the dlPFC are unilaterally independent such that the response to a bilateral lesion may be different in each hemisphere. Although the correlation between lesion size and density of PV-positive cells is high within either hemisphere, the significant increase in only left hemisphere PV-immunoreactive neuron density following hippocampal lesion adds support for the independent developmental influence of hippocampus on dlPFC in a given hemisphere. Additionally, estimations of the total

number of PV-immunoreactive cells within each hemisphere were consistent with our density findings. PV-positive estimated populations were increased in the Neo-H monkeys as compared to the Neo-C monkeys, as well as in the left hemisphere dlPFC when compared to the right hemisphere.

Relevant to our findings of altered levels of PV-positive interneurons, the lateralized hippocampal differences in humans with neurodevelopmental disorders are noteworthy. For instance, the left hippocampus is activated during verbal performance tasks and the right hippocampus is activated in response to nonverbal tasks (Hanlon, 2012). Consistent with such lateralization, a previous study found that the functional connectivity between the left hippocampal formation and the right dlPFC was disrupted during working memory tasks specifically in schizophrenics, although similar results between the right hippocampus-left dlPFC connection could not be confirmed (Meyer-Lindenberg et al., 2005). Impairment of the hippocampus to dlPFC functional connectivity is present in other neurodevelopmental disorders including major depression. For instance, Geng et al. (2016) reported significant bilateral structural and functional disruption to the hippocampus-PFC circuit in first episode MDD patients as compared to neurotypical controls.

Further, as outlined in the Introduction, humans with schizophrenia present major volumetric alterations of the hippocampus. For instance, longitudinal studies of schizophrenics found that the volume of the hippocampus within the left hemisphere specifically was reduced compared to volume at symptom onset (Rizos, 2014). Interestingly, work on human schizophrenia patients demonstrated a reduction in gamma-oscillation amplitude during working memory tasks as compared to a control group (Chen et al., 2014). The same research found a strong correlation between gamma-oscillation amplitude and the level of left dlPFC GABA

among the experimental group. This finding is interesting in light of our own finding that neonatal hippocampal lesion in rhesus monkeys increased cortical GABA confined to the left hemisphere.

While it remains unclear why the left hippocampus is differentially affected by schizophrenia, our results were consistent with an increased impact to dlPFC following hippocampal lesion in the left hemisphere. In human studies, the left hemisphere has been implicated specifically in verbal working memory tasks which are not present in monkey models but do require a large amount of memory processing and monitoring (Petersson, Gisselgard, Gretzer, and Ingvar, 2006; Nagel, Herting, Maxwell, Bruno, and Fair, 2013). While monkeys do not talk, they do vocalize and PV cells may be key drivers of oscillations that lay the foundation for communication (Thut, 2014; Tikidji-Hamburyan, Martinez, White, and Canavier 2015). A disruption to these oscillations may impact the ability for a monkey to monitor vocalizations similar to behavioral deficits in working memory monitoring shown in our monkeys.

Limitations

While the results of this study were informative, all the data should be interpreted with regard to several limitations. First, these results should only be interpreted as part of a model of early insult pathogenesis of schizophrenia, as they do not relate to other aspects of schizophrenia pathology. In addition, one of the primary methodological issues was the incompleteness of lesions of the hippocampus which may lead to an underestimation of the effect of lesion on dlPFC development. This said, the lesions more closely mimic the extent of real-world lesions that may contribute to schizophrenia. For the purpose of this project, though, we were able to make interesting inferences regarding the differences in lesion size. For example, we found a

strong, positive correlation between the percent of hippocampus lesioned as determined by Bachevalier and Heuer (2011) and PV cell density.

In terms of the actual tissue, we tried to control for differences in staining by always running Neo-H and Neo-C tissue simultaneously. That said, slight differences existed in quality of staining between cases. Another variable that we tried to control for was the shrinkage that is characteristic of post-mortem tissue processing which may have affected our tissue and thus our stereological counts slightly (Figure 10).

Finally, the sample used was small in comparison to other biological investigations. While our project was consistent with procedures from other studies using non-human primate models and our coefficient of error suggests that we used an adequate number of sections and counts, analysis of additional monkeys will be useful in confirming the specific patterns found in this research.

Functional significance

Our anatomical and morphological analysis of the dlPFC can be correlated with specific behavioral data in order to determine the role PFC plays in diminished working memory (Petrides, 1995). Specifically, behavioral research performed on the monkeys used in this project by the Bachevalier Lab suggests that neonatal hippocampal lesions selectively impair working memory processes (Heuer and Bachevalier, 2011). The research tested the animals on a Session-Unique Delayed Nonmatching-to-Sample Task (SU-DNMS) and an Object Self-Ordered Task (Obj-SO). The SU-DNMS task is an established means of testing maintenance of information as part of working memory while the Obj-SO task is a means of measuring information monitoring. While monkeys with neonatal damage to the hippocampus did not deviate from healthy controls on the SU-DNMS task, the lesioned monkeys were severely impaired on the Obj-SO (all

lesioned monkey data reported in Appendix). This suggests that an early hippocampal lesion may impact the monkeys' ability to monitor self behavior on successive tasks. Because there exists substantial overlap in the roles of the hippocampus and PFC, it is not clear whether the damage to the hippocampus or the resulting maldevelopment of the PFC was cause of disrupted working memory (Heuer and Bachevalier, 2011).

Although this work may be considered basic science research, our results have implications for a better understanding of how early life lesion of hippocampus may affect vulnerable structures with implications for disrupting normal behavior and cognition. Such lesions may be the result of severe malnutrition in utero, a difficult birth that restricts oxygen to the baby, a car accident, a fall or any number of similar stress events (NIMH, 2016). Our research is significant in that little to no work has been done to investigate the anatomical repercussions of neonatal hippocampal lesions in the rhesus monkey brain. As our anatomical data and the behavioral data compiled by the Bachevalier Lab suggest, neonatal insult to the hippocampus may disrupt the dlPFC's GABAergic circuitry, and thus an individual's ability to perform working memory tasks in adulthood. While working memory is integral to neurotypical human activity, research has established a link between working memory performance and neurodevelopmental disorders including schizophrenia, such that working memory deficits may ultimately be utilized as an endophenotypic marker of schizophrenia (Park and Gooding, 2014).

Further, while lesion studies have been extremely useful in establishing a link between brain regions and functions, structural analysis of relevant ROIs can help support an understanding of the mechanisms behind dysfunction (Damasio, 1994; Bachevalier, Beauregard, and Alvarado, 1999; Silvanto, 2015). Ultimately, similar exploratory research cannot be performed in humans for both ethical and methodological reasons including an inability to

control for confounding variables as was possible in our project. Thus, as scientists, our inquiry must utilize the next best model, in hopes of providing valuable information that could potentially build a more comprehensive understanding of the brain and its complex circuitry.

Conclusions

Ultimately, our research findings are consistent with the current body of research that suggests a relationship between the hippocampus and the development of GABAergic circuitry within the dorsolateral prefrontal cortex. While our results did not support our original hypothesis that hippocampal lesions would result in bilateral reduction of PV interneurons, they did demonstrate that the number of GABAergic parvalbumin-positive cells increase in the left hemisphere dlPFC of monkeys that sustained neonatal hippocampal lesions. These findings are consistent with work done by the Bachevalier lab which found working memory deficits in these monkeys and with work performed in human patients which found volumetric differences isolated to the left hippocampus (Rizos, 2014; Kawano, 2015). Because we generated significant results using a small sample size, future projects expanding on the number of monkeys and antibodies may provide a more comprehensive understanding of GABAergic development within the prefrontal cortex. A significant amount of valuable information may be gained from rhesus monkey lesion studies of this nature, allowing for a better understanding of GABAergic circuitry in the developing dlPFC and its relation to neurodevelopmental disorder etiology.

Future directions

The data gathered as part of this research project are informative and have led our research team to explore future options and offer suggestions for the future research of others. Because our sample size included only eight monkeys, we will analyze additional monkeys that

have been reared for this project. In addition, we will continue to explore further antigen retrieval manipulations to visualize the neuro-markers that proved elusive to this point. Although our attempts have thus far been mostly unsuccessful, we believe that the proper combination of antibody, dilution, antigen retrieval, and wash buffer will allow us to properly visualize structures of interest. The antibodies used thus far were not generated specifically for rhesus monkeys, meaning that finding an antibody with similar enough amino acid homology may require a combination of greater luck and market interest among other things. Furthermore, while this issue presented a complication for the project, the investigation into antigen retrieval protocols provided the opportunity to more deeply grapple with and understand issues of IHC, as well as experience first-hand that scientific inquiry can be limited by any number of variables (Figure 23).

While the visualization and analysis of PV, Cal, SST, and GRα2 can give us a strong understanding of the GABAergic circuitry generated by our research paradigm, more markers will need to be analyzed and worked out in order to provide a comprehensive understanding of the development of dlPFC GABAergic circuitry following lesion of the hippocampus. While some of these additional markers will be GABAergic in nature, it will be interesting to also compare analyses of non-GABAergic neuro-markers including Tyrosine Hydroxylase, a catecholamine synthesizing enzyme. In addition, an analysis of the ratio of parvalbumin cells to pyramidal cells in our region of interest remains an active pursuit as this analysis would indicate the relative level of inhibitory signaling and excitatory cortical output. Similarly, we plan to expand this analysis to other cortical regions to assess whether our results are confined to Layer IIIA or are more ubiquitous.

Lastly, other regions within the PFC, notably the vmPFC, are ideal candidates for anatomical analyses following neonatal hippocampal lesion. While the dlPFC is the primary region within the rhesus monkey and human cortex responsible for working memory, regions involved in other executive tasks may be interesting to analyze (Blue, Kazama, and Bachevalier, 2013). Specifically, the vmPFC has been implicated in emotional decision making, such that pre-sacrifice behavioral tasks with emotional valence could be paired with an anatomical analysis to better understand the role of the hippocampus in vmPFC development (Bechara, Tranel, and Damasio, 2000). Further, since the hippocampus to vmPFC connection is monosynaptic, we hypothesize that there will exist a similar, or likely even more pronounced, GABAergic deficit in this region (Nieuwenhuis and Takashima, 2011).

References

"Antigen Retrieval Methods, Techniques, Protocols." Antigen Retrieval Methods, Techniques, Protocols. IHC World, 2011. Web. 15 Feb. 2016. http://www.ihcworld.com/epitope_retrieval.htm

Altunkaynak, B.Z. (2012). A brief introduction to stereology and sampling strategies: basic concepts of stereology. NeuroQuantology. Vol 10. (1). 31-43.

Auger, M.L. and Floresco, S.B. (2015). Prefrontal cortical gaba modulation of spatial reference and working memory. Int J Neuropsychopharmacol. 18(2).

Bachevalier, J., Beauregard, M., and Alvarado, M.C. (1999). Long-term effects of neonatal damage to the hippocampal formation and amygdaloid complex on object discrimination and object recognition in rhesus monkeys (Macaca mulatta). Behav Neurosci. 113(6):1127-51.

Barbas, H., and Blatt, G. (1995). Topographically specific hippocampal projections target functionally distinct hippocampal areas in the rhesus monkey, Hippocampus, (5)511-553.

Beasley, C.L., and Reynolds, G.P. (1997). Parvalbumin-immunoreactive neurons are reduced in the prefrontal cortex of schizophrenics. Schizophr Res. 24(3):349-55.

Beasley, C.L., and Zhang, Z.J. (2002). Selective deficits in prefrontal cortical GABAergic neurons in schizophrenia defined by the presence of calcium-binding proteins, Society of Biological Psychiatry. 52:708–715.

Bechara, A., Tranel, D., and Damasio, H. (2000). Characterization of the decision-making deficit of patients with ventromedial prefrontal cortex lesions. Brain 123 (11): 2189–202.

Becker, L.A. "Effect Size." Effect Size Calculators. UCCS, n.d. 21 Mar. 2000. Web. 17 Mar. 2016. http://www.uccs.edu/lbecker/effect-size.html

Bissonette, G.B., and Roesch, M.R. (2015). Neural correlates of rules and conflict in medial prefrontal cortex during decision and feedback epochs. Front Behav Neurosci. 9: 266.

Blue, S.N., Kazama, A.M., and Bachevalier, J. (2013). Development of memory for spatial locations and object/place associations in infant rhesus macaques with and without neonatal hippocampal lesions. Journal of the International Neuropsychological Society, 19, 1052-1064.

Bourgeois, J.P., Goldman-Rakic, P.S., and Rakic, P. (1994). Synaptogenesis in the prefrontal cortex of rhesus monkeys. Cereb Cortex. 4(1):78-96.

Breier, A., et al. (1997). Schizophrenia is associated with elevated amphetamine-induced synaptic dopamine concentrations: Evidence from a novel positron emission tomography method. Proc. Natl. Acad. Sci. 94. 2569–2574.

Callicott, J.H., et al. (2000). Physiological dysfunction of the dorsolateral prefrontal cortex in schizophrenia revisited. Cereb Cortex. 10(11):1078-92.

Chan, A.W., et al. (2015). Progressive cognitive deficit, motor impairment and striatal pathology in a transgenic Huntington's disease monkey model from infancy to adulthood. PLOS ONE. 10. (5).

Charych, E.I., Liu, F., Moss, S.J., and Brandon, N.J. (2009). GABAA receptors and their associated proteins: Implications in the etiology and treatment of schizophrenia and related disorders, Neuropharmacology. 57: 481-495.

Chaudhry, E.I., et al. (1998). The vesicular GABA transporter, vgat, localizes to synaptic vesicles in sets of glycinergic as well as GABAergic neurons. The Journal of Neuroscience. 18(23): 9733-9750.

Chen, C. A., et al. (2014). GABA level, gamma oscillation, and working memory performance in schizophrenia NeuroImage: Clinical 4 (2014) 531–539.

Chlan-Fourney, J., et al. Neonatal temporal lobe lesion disrupts prefrontal circuitry in monkeys. Manuscript.

Christensen, J.R., et al. (2007). Neocortical and hippocampal neuron and glial cell numbers in the rhesus monkey. The Anatomical Record. 290:330–340.

Clark, B.D., Goldberg, E.M., and Ruby, B. (2009). Electrogenic tuning of the axon initial segment. Neuroscientist. 15 (6): 651–668.

Clemmensen, L., Vernal, D.L., and Steinhausen, H.C. (2012). A systematic review of the long-term outcome of early onset schizophrenia. BMC Psychiatry.12:150.

Coefficient Theory | Stereology Information Center." Stereologyinfo. Mbf Bioscience, n.d. Web. 15 Mar. 2016. http://www.stereology.info/some-ce-theory/.

Conde, F., Lund, J.S., Jacobowitz, D.M., Baimbridge, K.G., and Lewis, D.A. (1994). Local circuit neurons immunoreactive for calretinin, calbindin d-28k or parvalbumin in monkey prefrontal cortex: distribution and morphology, Journal of Comparative Neurology. 341: 95-116.

Cruz, D.A., Eggan, S.M., and Lewis, D.A. (2003). Postnatal development of pre- and postsynaptic GABAmarkers at chandelier cell connections with pyramidal neurons in monkey prefrontal cortex. The Journal of Comparative Neurology. 465:385–400.

Damasio, H., Grabowski, T., Frank, R, Galaburda, A.M., and Damasio, A.R. (1994). The return of Phineas Gage: clues about the brain from the skull of a famous patient. Science. 264(5162):1102-5.

Davies, M. (2003). The role of GABAA receptors in mediating the effects of alcohol in the central nervous system. J Psychiatry Neurosci. 28(4): 263–274.

Deutsch, S.I., Rose, R.B., Schwartz, B.L., and Mastropaolo, J. (2001). A revised excitotoxic hypothesis of schizophrenia: therapeutic implications. Clin Neuropharmacol. 24(1):43-9.

"Effect Size." Effect Size Calculator. AI-Therapy: Statistics For Psychologists, n.d. Web. 16 Mar. 2016. https://www.ai-therapy.com/psychology-statistics/effect-size-calculator.

Fenalti, G., and Buckle, A.M. (2010). Structural biology of the GAD autoantigen. Autoimmunity Reviews. Volume 9, Issue 3. Pages 148–152.

Flores, C.E., et al. (2015). Activity-dependent inhibitory synapse remodeling through gephyrin phosphorylation. Proc Natl Acad Sci.112(1):65-72.

Garbutt, J.C., and van Kammen, D.P. (1983). The interaction between GABA and dopamine: implications for schizophrenia. Schizophr Bull. 9(3):336-53.

Geinisman, Y., deToledo-Morrell, L., Morrell, F., Persina, I.S., and Rossi, F.M. (1992). Age-related loss of axospinous synapses formed by two afferent systems in the rat dentate gyrus as revealed by the unbiased stereological dissector technique. Hippocampus. Vol 2. 4. 437-444.

Geng, H. et al. (2016). Disrupted structural and functional connectivity in prefrontal-hippocampus circuitry in first-episode medication-naïve adolescent depression. PLOS ONE 11(2).

Giannaris, E.L., and Rosene, D.L. (2012). A stereological study of the numbers of neurons and glia in the primary visual cortex across the lifespan of male and female rhesus monkeys. J Comp Neurol. 520(15).

Gill, K.M., and Grace, A.A. (2014). Corresponding decrease in neuronal markers signals progressive parvalbumin neuron loss in mam schizophrenia model. International Journal of Neuropsychopharmacology, 10: 1609-1619.

Girgis, R.R., et al. (2016). A proof-of-concept, randomized controlled trial of DAR-0100A, a dopamine-1 receptor agonist, for cognitive enhancement in schizophrenia. J Psychopharmacol. [Epub ahead of print].

Gonchar, Y., Turney, S., Price, J.L., and Burkhalter, A. (2002). Axo-axonic synapses formed by somatostatin-expressing GABAergic neurons in rat and monkey visual cortex. J Comp Neurol. 2002 Jan 28;443(1):1-14.

Gonzalez-Burgos, G. and Lewis, D.A. (2012). NMDA receptor hypofunction, parvalbumin-positive neurons, and cortical gamma oscillations in schizophrenia. Schizophr Bull. 2012 Sep; 38(5): 950–957.

Gordon, J.A. (2010). Testing the glutamate hypothesis of schizophrenia. Nature Neuroscience, 13, 2-4.

Gundersen, H.J. (1986). Stereology of arbitrary particles. A review of unbiased number and size estimators and the presentation of new ones in memory of William J Thompson. J Microsc. 143. 3-45.

Hanlon, F.M., et al. (2012). Fronto-temporal anatomical connectivity and working-relational memory performance predict everyday functioning in schizophrenia. Psychophysiology. 49(10): 1340–1352.

Hayes, D.J. (2015). GABAergic circuits underpin valuative processing. Front. Syst. Neurosci. 9:76.

Heuer, E. and Bachevalier, J. (2011). Neonatal hippocampal lesions in rhesus macaques alter the monitoring, but not maintenance, of information in working memory. Behavioral Neuroscience. Vol. 125, No. 6, 859–870.

Hirata, Y., et al. (2003). Dorsal area 46 is a major target of disynaptic projections from the medial temporal lobe. Cerebral Cortex. 23:2965–2975.

Hoffman, R.E., et al. (2003). Transcranial magnetic stimulation of left temporoparietal cortex and medication-resistant auditory hallucinations. Archives of General Psychiatry. 60: 49-56.

Huang, J. et al. (2014). Working memory dysfunctions predict social problem solving skills in schizophrenia. Psychiatry Res. 220(1-2):96-101.

Isseroff, A., Rosvold, H.E., Galkin, T.W., and Goldman-Rakic, P.S. (1982). Spatial memory impairments following damage to the mediodorsal nucleus of the thalamus in rhesus monkeys. Brain Research, 232, 97–113.

Johnston, G.A. (1996). GABAA receptor pharmacology. Pharmacology and Therapeutics 69 (3): 173–198.

Kantrowitz, J., Citrome, L., and Javitt, D. (2009). GABA(B) receptors, schizophrenia and sleep dysfunction: a review of the relationship and its potential clinical and therapeutic implications. NS Drugs. 23(8):681-91.

Kaplan, S. et al. (2012). The disector counting technique. NeuroQuantology. 10 (1). 44-53.

Kawaguchi, Y. and Kubota, Y. (1997). GABAergic cell subtypes and their synaptic connections in rat frontal cortex. Cereb Cortex. 7(6):476-86.

Kawano, M. et al. (2015). Hippocampal subfield volumes in first episode and chronic schizophrenia. PLoS One. 10(2).

Kelsum, C., and Lu, W. (2013). Development and specification of GABAergic cortical interneurons. Cell & Bioscience. 3:19.

Keuker, J.I., Luiten P.B., and Fuchs, E. (2003). Preservation of hippocampal neuron numbers in aged rhesus monkeys. 24(1):157-65.

Kilb, W. (2012). Development of the GABAergic system from birth to adolescence. The Neuroscientist 18(6) 613–630.

Kim, J.J., et al. (2003). Functional disconnection between the prefrontal and parietal cortices during working memory processing in schizophrenia: A[15(O)]H2O PET study. *American Journal of Psychiatry, 160,* 919–923.

Kruger, H.S., Brockmann, M.D., Salamon, J., Ittrich, H, and Hanganu-Opatz, I.L. (2012). Neonatal hippocampal lesion alters the functional maturation of the prefrontal cortex and the early cognitive development in pre-juvenile rats. Neurobiol Learn Mem. 97(4):470-81.

Kuhn, J. et al. (2014). Deep brain stimulation in schizophrenia. Nervosa Superior. 56, No. 3.

Lazarus, R.S. (1993). From psychological stress to the emotions: A history of changing outlooks. Annual Review of Psychology 44 (1): 1–21.

Lawrie, S.M. and Abukmeil, S.S. (1998). Brain abnormality in schizophrenia. A systematic and quantitative review of volumetric magnetic resonance imaging studies. Br J Psychiatry. 172:110–120.

Lewine, R.R., Hudgins, P., Brown, F., Caudle, J., and Risch, S. (1995). Differences in qualitative brain morphology findings in schizophrenia, major depression, bipolar disorder, and normal volunteers. Schizophrenia Research. 15(3):253-9.

Lewis, D.A., and Hashimoto, T. (2007). Deciphering the disease process of schizophrenia: The contribution of cortical GABA neurons, International Review of Neurobiology, Vol. 78, 78:109-131.

Lewis, D.A., Hashimoto, T., and Volk, D.W. (2005). Cortical inhibitory neurons and schizophrenia Nature Reviews Neuroscience. 4. 312-324.

McClintock, S.M., Freitas. C., Oberman, L., Lisanby, S.H., and Pascual-Leone, A. (2011). Transcranial magnetic stimulation: a neuroscientific probe of cortical function in schizophrenia. Biol Psychiatry 70:19–27.

Melchitzky, D.S., and Lewis, D.A. (2008). Dendritic-targeting GABA neurons in monkey prefrontal cortex: comparison of somatostatin- and calretinin-immunoreactive axon terminals. Synapse. 62(6):456-65.

Meng, Y. et al. Decreased functional connectivity in dorsolateral prefrontal cortical networks in adult macaques with neonatal hippocampal lesions: relations to visual working memory deficits. Manuscript.

Merrill, D.A., Roberts, J.A., and Tuszynski, M.H. (2000). Conservation of neuron number and size in entorhinal cortex layers II, III, and V/VI of aged primates. J Comp Neurol. 422(3):396-401.

Meyer-Lindenberg, A.S., et al. (2005). Regionally specific disturbance of dorsolateral prefrontal–hippocampal functional connectivity in schizophrenia. Arch Gen Psychiatry. 2005;62(4):379-386.

Morecraft, R.S., et al. (2013). terminal distribution of the corticospinal projection from the hand/arm region of the primary motor cortex to the cervical enlargement in rhesus monkey. J Comp Neurol. 521(18): 4205–4235.

Morecraft, R.J., Stillwell-Morecraft, K.S., Solon-Cline, K.M., Ge, J., and Darling, W.G. (2014). Cortical innervation of the hypoglossal nucleus in the non- human primate (Macaca mulatta). J Comp Neurol. 522(15): 3456–3484.

Morris, H.M., Hashimoto, T., and Lewis, D.A. (2008). Alterations in somatostatin mRNA expression in the dorsolateral prefrontal cortex of subjects with schizophrenia or schizoaffective disorder. Cerebral Cortex. 18:1575—1587.

Murray A.J, et al. (2015). Parvalbumin-positive interneurons of the prefrontal cortex support working memory and cognitive flexibility. Sci Rep. 2015; 5: 16778.

Nagel, B.J., Herting, M.M., Maxwell, E.C., Bruno, R., and Fair, D. (2013). Hemispheric lateralization of verbal and spatial working memory during adolescence. Brain Cogn. 82:58–68.

Nakahara, K., Adachi, Y., Osada, T., and Miyashita, Y. (2007). Exploring the neural basis of cognition: multi-modal links between human fMRI and macaque neurophysiology. Trends Cogn Sci. 11(2):84–92.

Nakazawa et al. (2012). GABAergic interneuron origin of schizophrenia pathophysiology. Neuropharmacology. 62(3): 1574–1583.

Nelson, M.D., Saykin, A.J., Flashman, L.A., and, Riordan, H.J. (1998). Hippocampal volume reduction in schizophrenia as assessed by magnetic resonance imaging: a meta-analytic study. Arch Gen Psychiatry 55:433–440.

Nie, H., Graven-Nielsen, T., and Arendt-Nielsen, L. (2009). Spatial and temporal summation of pain evoked by mechanical pressure stimulation. European Journal of Pain 13 (6): 592–599.

Nieuwenhuis, I.L. and Takashima, A. (2011). The role of the ventromedial prefrontal cortex in memory consolidation. Behav Brain Res. (2):325-34.

NIMH. U. S. Department of Health and Human Services, National Institutes of Health, National Institute of Mental Health. Mental Health Information. Schizophrenia. 2016.

Nutt, D. (2006). GABAA receptors: subtypes, regional distribution, and function. Journal of Clinical Sleep Medicine, Vol. 2, No. 2.

O'Donnell, K.A., Rapp, P.R., and Hof, P.R. (1999). Preservation of prefrontal cortical volume in behaviorally characterized aged macaque monkeys. Exp Neurol. 160(1):300-10.

O'Donnell, K.A. (2012). Cortical disinhibition in the neonatal ventral hippocampal lesion model of schizophrenia: new vistas on possible therapeutic approaches. Pharmacology and Therapeutics, 133, 19-25.

Olejnik, S. and Algina, J. (2003). Generalized eta and omega squared statistics: measures of effect size for some common research designs. Psychological Methods. Vol. 8, No. 4, 434–447.

Olney, J.W., and Farber, N.B. (1995). Glutamate receptor dysfunction and schizophrenia. Arch Gen Psychiatry. 52:998–1007.

Olsen, R.W., and DeLorey, T.M. (1999). GABA receptor physiology and pharmacology. Basic Neurochemistry: Molecular, Cellular and Medical Aspects. 6th edition. Philadelphia: Lippincott-Raven.

Optical Disector | Stereology Information Center. Stereologyinfo. Mbf Bioscience, n.d. Web. 15 Mar. 2016. http://www.stereology.info/optical-disector/.

Optical Fractionator | Stereology Information Center. Stereologyinfo. Mbf Bioscience, n.d. Web. 15 Mar. 2016. http://www.stereology.info/the-optical-fractionator/.

Ouellet, L. and de Villers-Sedani, E. (2014). Trajectory of the main GABAergic interneuron populations from early development to old age in the rat primary auditory cortex. Front Neuroanat. 8: 40.

Park, S., and Gooding, D.C. (2014). Working memory impairment as an endophenotypic marker of a schizophrenia diathesis. Schizophr Res Cogn. 1(3):127-136.

Passingham, R. (2009). How good is the macaque monkey model of the human brain? Curr Opin Neurobiol. 19(1): 6–11.

Payne, C., Machado, C.J., Bliwise, N.G., and Bachevalier, J. (2010). Maturation of the hippocampal formation and amygdala in Macaca mulatta: A volumetric magnetic resonance imaging. Hippocampus. 20(8): 922–935.

Perova, Z., Delevich, K., and Li, B. (2015). Depression of excitatory synapses onto parvalbumin interneurons in the medial prefrontal cortex in susceptibility to stress. J Neurosci. 35(7):3201-6.

Perry, W., Geyer, M.A., and Braff, M.L. (1999). Simultaneous measurement of information processing and thought disorder in schizophrenia. Archives of General Psychiatry, 56:277-281.

Peters, A., Leahu, D., Moss, M.B., and McNally, K.J. (1994). The effects of aging on area 46 of the frontal cortex of the rhesus monkey. Cerebral Cortex. 6:621-635.

Petrides, M. (1995). Impairments on nonspatial self-ordered and externally ordered working memory tasks after lesions of the mid-dorsal part of the lateral frontal cortex in the monkey. Journal of Neuroscience, 15, 359 –375.

Petrides, M., and Pandya, D.N. (1999). Dorsolateral prefrontal cortex: comparative cytoarchitectural analysis in the human and macaque brain and corticocortical connection patterns. European Journal of Neuroscience. 11. 1011-1036.

Petersson, K.M., Gisselgard, J., Gretzer, M., and Ingvar, M. (2006). Interaction between a verbal working memory network and the medial temporal lobe. Neuroimage. 33:1207–1217.

Picchioni, M.M. and Murray, R.M. (2007). "Schizophrenia". BMJ 335 (7610): 91–95.

Piper, M., et al. (2012). The neurodevelopmental hypothesis of schizophrenia: convergent clues from epidemiology and neuropathology. Psychiatr Clin North Am. 35(3):571-84.

Preuss, T.M., and Goldman-Rakic, P.S.(1991). Myelo- and cytoarchitecture of the granular frontal cortex and surrounding regions in the strepsirhine primate galago and the anthropoid primate Macaca. The Journal of Comparative Neurology. 310:429-474.

Regier, D.A., Narrow, W.E., Rae, D.S., Manderscheid, R.W., Locke, B.Z., Goodwin, F.K. (1993). The de facto US mental and addictive disorders service system. Epidemiologic catchment area prospective 1-year prevalence rates of disorders and services. Arch Gen Psychiatry 50:85–94.

Reynolds, G.P., and Beasley, C.L. (2001). GABAergic neuronal subtypes in the human frontal cortex-development and deficits in schizophrenia. J Chem Neuroanat. 22(1-2):95-100.

Raghanti, M.A., et al. (2008). Cortical dopaminergic innervation among humans, chimpanzees, and macaque monkeys: A comparative study Neuroscience. 155(1): 203–220.

Rishi, R., Sinha, A., and Radhakrishna, S. (2013). Comparative demography of two commensal macaques in india: implications for population status and conservation. Folia Primatologica 84: 384–393.

Rizos, E. et al. (2014). A longitudinal study of alterations of hippocampal volumes and serum BDNF levels in association to atypical antipsychotics in a sample of first-episode patients with schizophrenia. PLoS One. 9(2).

Rodman, H.R., Sorenson, K.M., Shim, A.J., and Hexter, D.P. (2001). Calbindin immunoreactivity in the geniculo-extrastriate system of the macaque: implications for heterogeneity in the koniocellular pathway and recovery from cortical damage. J Comp Neurol. 431(2):168-81.

Rudy, B., Fishell, G., Lee, S., and Hjerling-Leffler, J. (2011). three groups of interneurons account for nearly 100% of neocortical gabaergic neurons. Dev Neurobiol. 71(1): 45–61.

Safronov, B.V., Wolff, M. and Vogel, W. (1999). Axonal expression of sodium channels in rat spinal neurons during postnatal development. J Physiol. 514 (3): 729–34.

Saleem, K.S. and Logothetis, N.K. A combined MRI and histology atlas of the rhesus monkey brain in stereotaxic coordinates. Academic Press, 2006. 9780080467771.

Scheaffer, R.L., Witmer, J., Watkins, A., and Gnanadesikan, M. (1996). Activity-Based Statistics. New York: Springer-Verlag.

Schlessinger, A., et al. (2012). High selectivity of the γ-aminobutyric acid transporter 2 (GAT-2, SLC6A13) revealed by structure-based approach. J Biol Chem. 287(45): 37745–37756.

Sekar, A., et al. (2016). Schizophrenia risk from complex variation of complement component 4. Nature. 130. 177-183.

Selten, J.P., Cantor-Graae, E., and Kahn, R.S. (2007). Migration and schizophrenia. Current Opinion in Psychiatry. 20 (2): 111-115.

Sesack, S.R., Snyder, C.L., and Lewis, D.A. (1995). Axon terminals immunolabeled for dopamine or tyrosine hydroxylase synapse on GABA-immunoreactive dendrites in rat and monkey cortex. J Comp Neurol. 363(2):264-80.

Sesack, S.R., Hawrylak, V.A., Melchitzky, D.S., and Lewis, D.A. (1998). Dopamine innervation of a subclass of local circuit neurons in monkey prefrontal cortex: ultrastructural analysis of tyrosine hydroxylase and parvalbumin immunoreactive structures. Cereb Cortex. 8:614-622.

Silvanto, J. (2015). Why is "blindsight" blind? A new perspective on primary visual cortex, recurrent activity and visual awareness. Conscious Cogn. 32:15-32.

Soghomonian, JJ. and Martin, D.L. (1998). Two isoforms of glutamate decarboxylase: why? Trends Pharmacol Sci. 19 (12): 500-5.

Squires, R.F., and Saederup, E. (1991). A review of evidence for GABergic predominance/glutamatergic deficit as a common etiological factor in both schizophrenia and affective psychoses: more support for a continuum hypothesis of "functional" psychosis. Neurochem Res.16(10):1099-111.

Steeds, H., Carhart-Harris, R.L., and Stone, J.M. (2015). Drug models of schizophrenia. Ther Adv Psychopharmacol. 5(1): 43–58.

Stereo Investigator Users Guide. mbf Bioscience. Print. Version 8. 2008.

Sugino, K., et al. (2006). Molecular taxonomy of major neuronal classes in the adult mouse forebrain. Nat. Neurosci. 9 (1): 99–107.

Sullivan, G.M., and Feinn, R.. (2012). Assessing effect size—or why the p value is not enough. J Grad Med Educ. 4(3): 279–282.

Szabadics, J. et al. (2006). Excitatory effect of GABAergic axo-axonic cells in cortical microcircuits. Science. Vol. 311, Issue 5758, pp. 233-235.

Tessner, K.D. Mittal, V., and Walker, E.F. (2011). Longitudinal study of stressful life events and daily stressors among adolescents at high risk for psychotic disorders. Schizophr Bull. 37(2): 432–441.

Thompson, J.L., Pogue-Geile, M.F., and Grace, A.A. (2004). Developmental pathology, dopamine, and stress: a model for the age of onset of schizophrenia symptoms. Schizophrenia Bulletin. 30 (4). 875-900.

Thut, G. (2014). modulating brain oscillations to drive brain function. PLoS Biol. 12(12).

Tikidji-Hamburyan, R.A., Martinez, J.J., White, J.A., and Canavier, C.C. (2015). Resonant interneurons can increase robustness of gamma oscillations. J Neurosci. 25;35(47):15682-95.

Timmins, R.J., Richardson, M., Chhangani, A., and Yongcheng, L. (2008). Macaca mulatta. IUCN Red List of Threatened Species. International Union for Conservation of Nature.

Volk, D.W., Austin, M.C., Pierri, J.N., Sampson, A.R., and Lewis, D.A. (2000). Decreased glutamic acid decarboxylase67 messenger RNA expression in a subset of prefrontal cortical gamma-aminobutyric acid neurons in subjects with schizophrenia. Arch Gen Psychiatry. 57:237–245.

Ward, T.S., Rosen, G.D., and Von Bartheld, C.S. (2008). Optical disector counting in cryosections and vibratome sections underestimates particle numbers: effects of tissue quality. Microsc Res Tech. (1): 60–68.

Weinberger, D.R., (1987). Prenatal origin of schizophrenia in a subgroup of discordant monozygotic twins. Archives of General Psychiatry. 44 (7). 660-669.

Zahn, L.M., Jasny, B.R., Culotta, E., and Pennisi, E. (2007). A barrel of monkey genes. Science 316 (5822): 215.

Zhou, Y. and Danbolt, N.C. (2013). GABA and glutamate transporters in brain. Front Endocrinology. 4: 165.

Figures

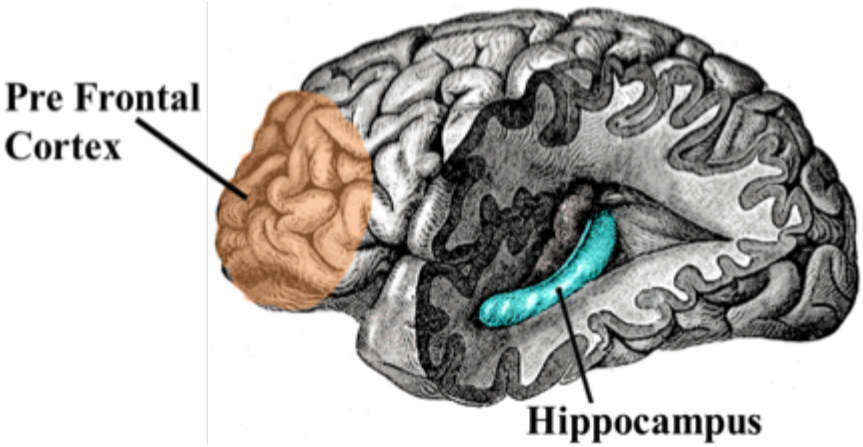

Figure 1: Macroscopic view of the location of the hippocampus (light blue) in relation to the Prefrontal Cortex (light orange). Both monosynaptic and disynaptic circuits connect the two regions.

Figure 2: Coronal section of rhesus monkey brain showing location of dorsolateral prefrontal cortex (dlPFC, red box), located within the upper bank of the principal sulcus.

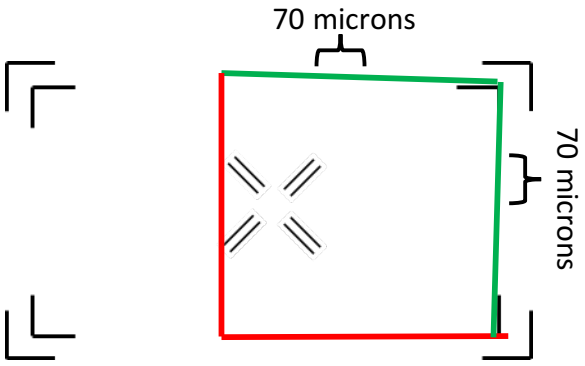

Figure 3: Photo reticle used for all cell counts. The green lines represent inclusion boundaries, where cells were counted if they fell within the line or had at least half of the total area on the line. The red lines represent exclusion boundaries whereby cells were not counted if they fell on, or outside these lines.

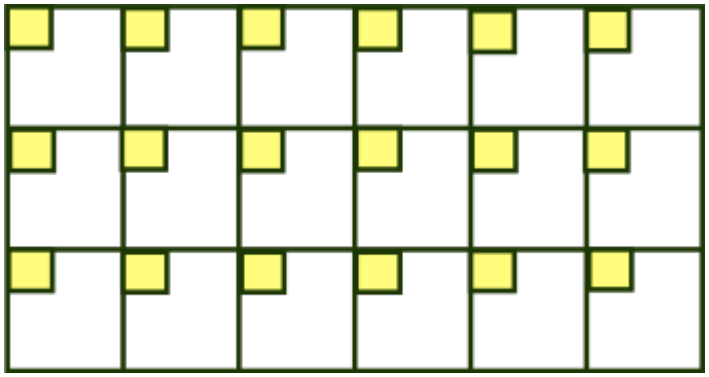

Figure 4: Our method of stereology utilized the optical fractionator technique. In conjunction with software, a transparency of the above was laid over a computer screen to allow for random, systematic counts.

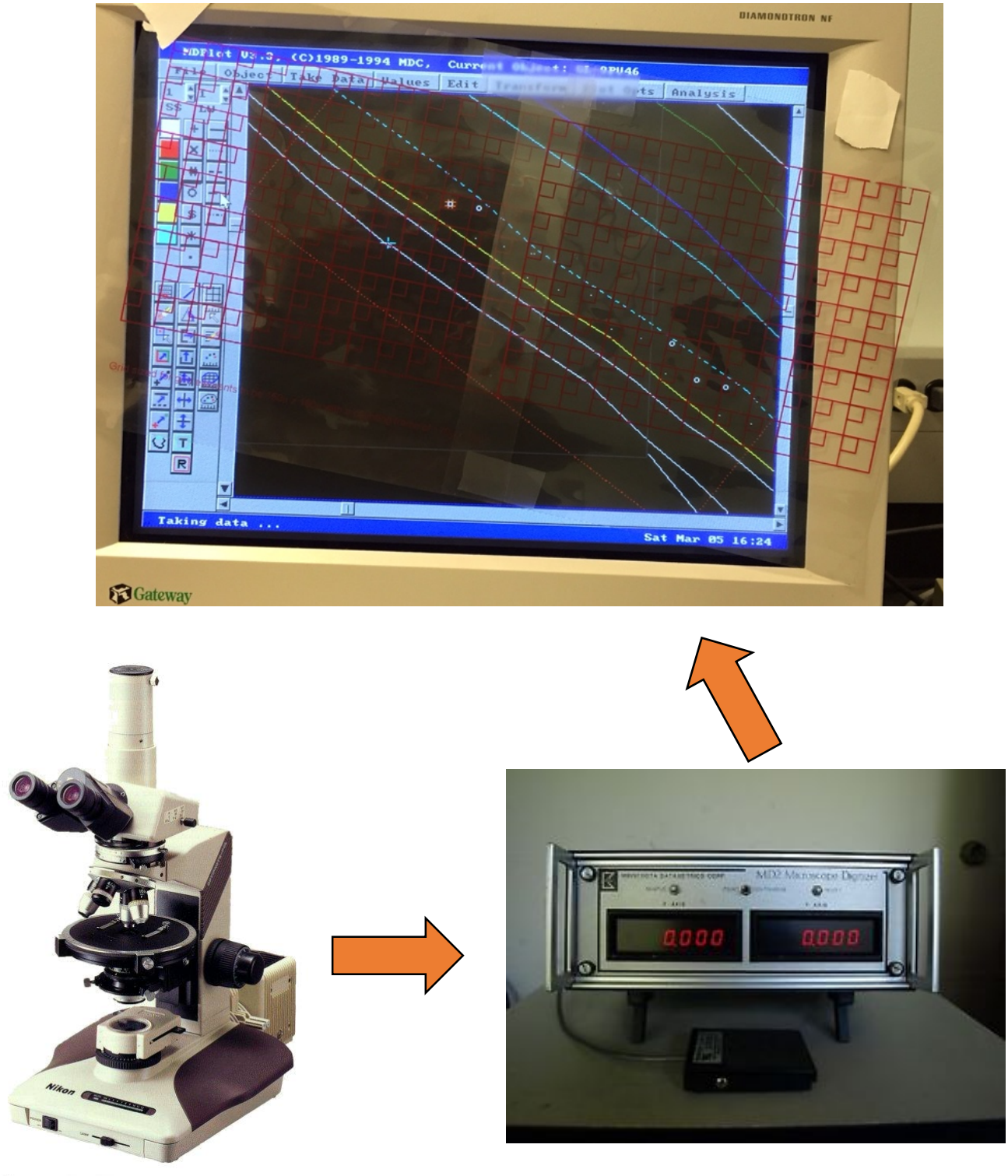

Figure 5: Stereological setup. The sampling grid and counting frame laid on the computer monitor showing the layers of cortex (Layer IIIA is yellow line to blue dotted line). As the microscope slide stage was moved, spatial information was sent to the Minnesota Datametrics hardware and ultimately virtually represented on screen. This setup allowed for systematic, random sampling of the region of interest.

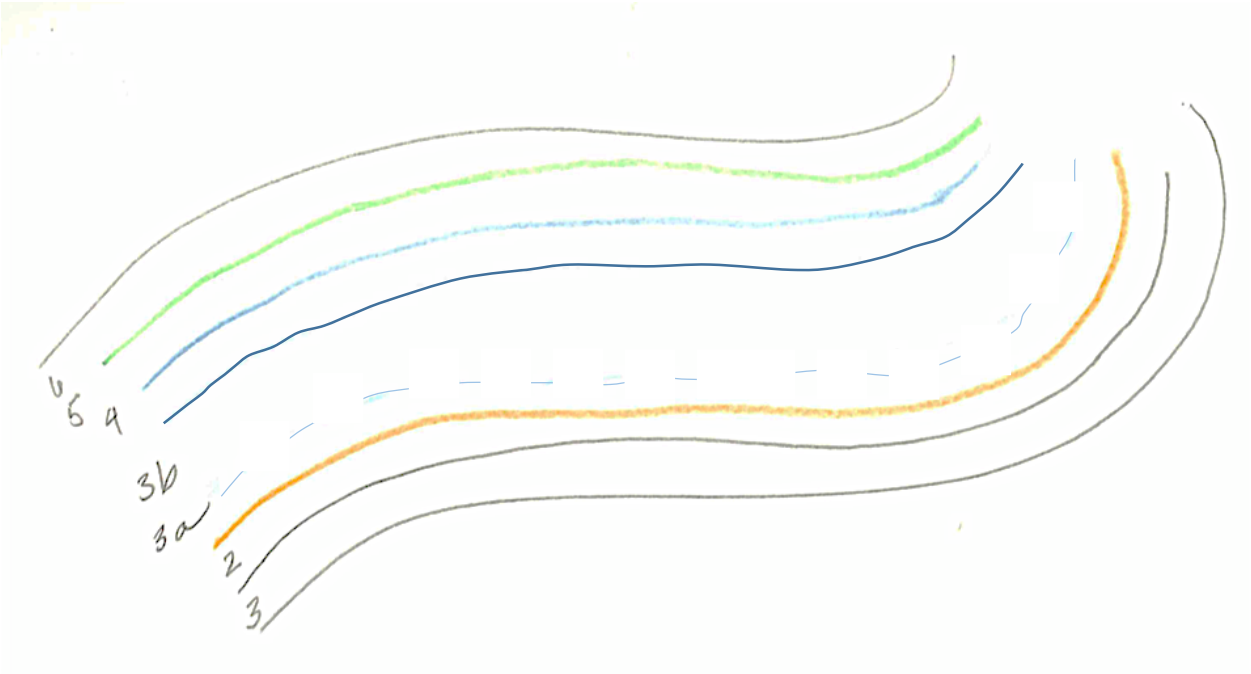

Figure 6: The traced layers of the upper bank of the principal sulcus. Counts were made using a counting frames within a sampling grid laid over Layer IIIA, demarcated as the space between the yellow and dotted blue line.

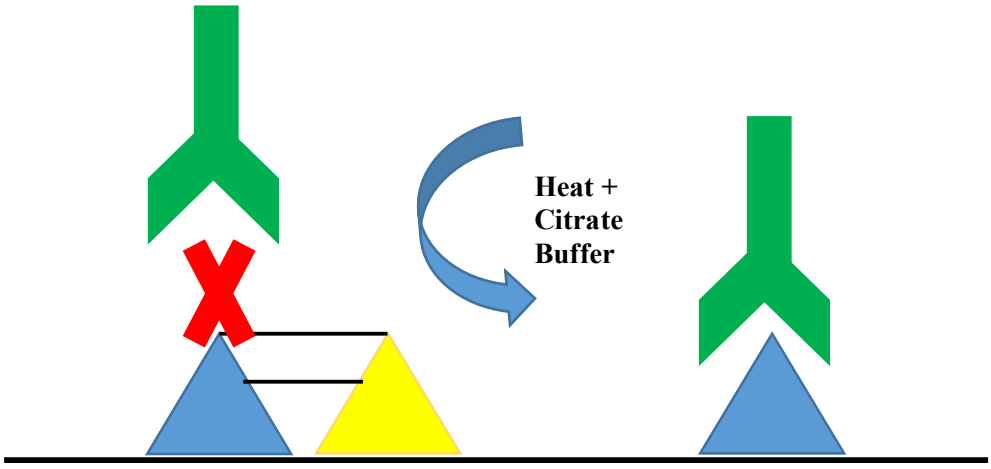

Figure 7: Heat-induced epitope retrieval. Crosslinks between two antigens can prevent an antibody (green) from binding its target antigen (blue). Heat-induced epitope retrieval (HIER), the exposure to relatively intense heat prior to IHC, may destroy these crosslinks and allow desired binding. The proteolytic-induced epitope retrieval (PIER) method of antigen retrieval works under a similar set of principles but uses an enzyme instead of heat in order to break the crosslinks between antigens.

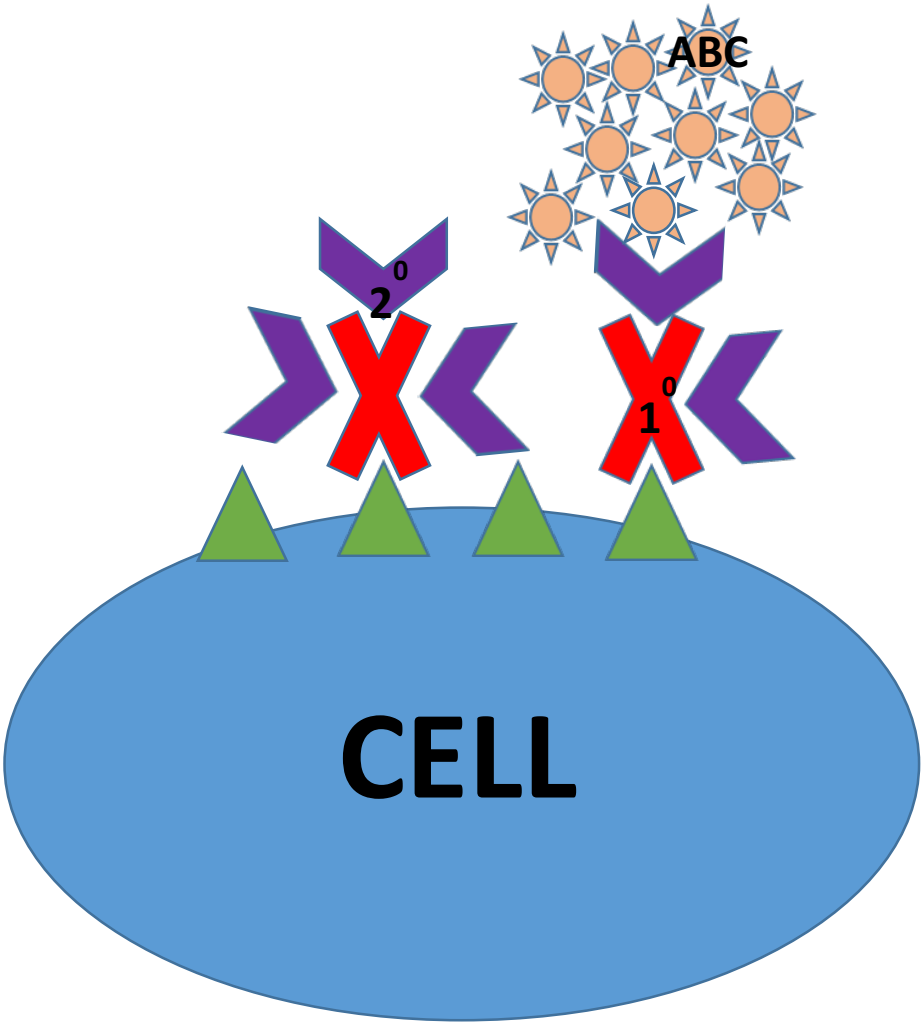

Figure 8: Immunohistochemistry involves the binding of a primary antibody (red X's) to specific antigens (green triangles) presented by the cell. A secondary antibody (purple chevrons) is then bound. Finally, the avidin-biotin method (ABC, orange suns) is applied for additional application.

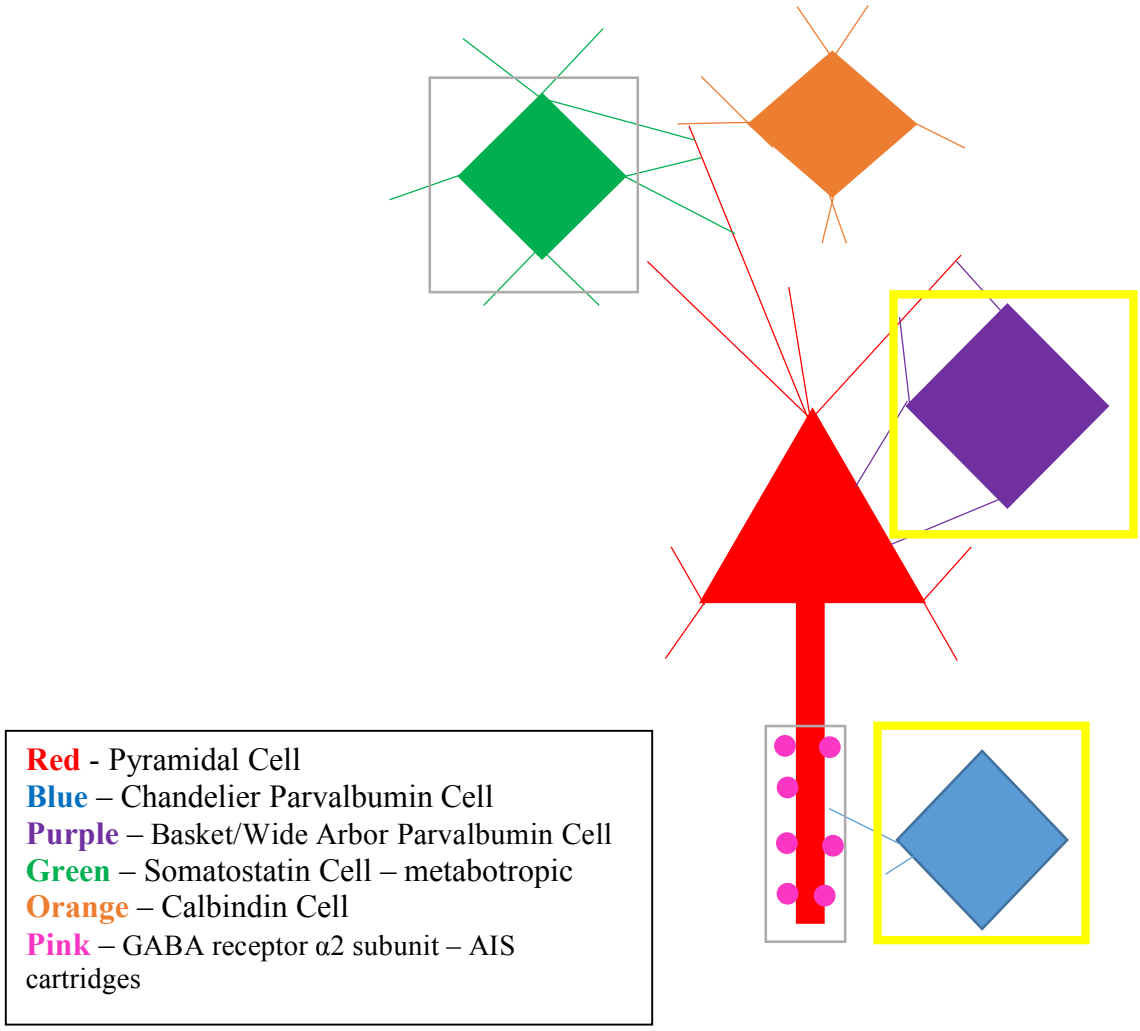

Figure 9: The understood GABAergic connections onto a given pyramidal cell within the frontal cortex. Cells we were able to visualize are indicated by a yellow box and those we attempted to visualize but have thus far been unsuccessful are indicated by a grey box.

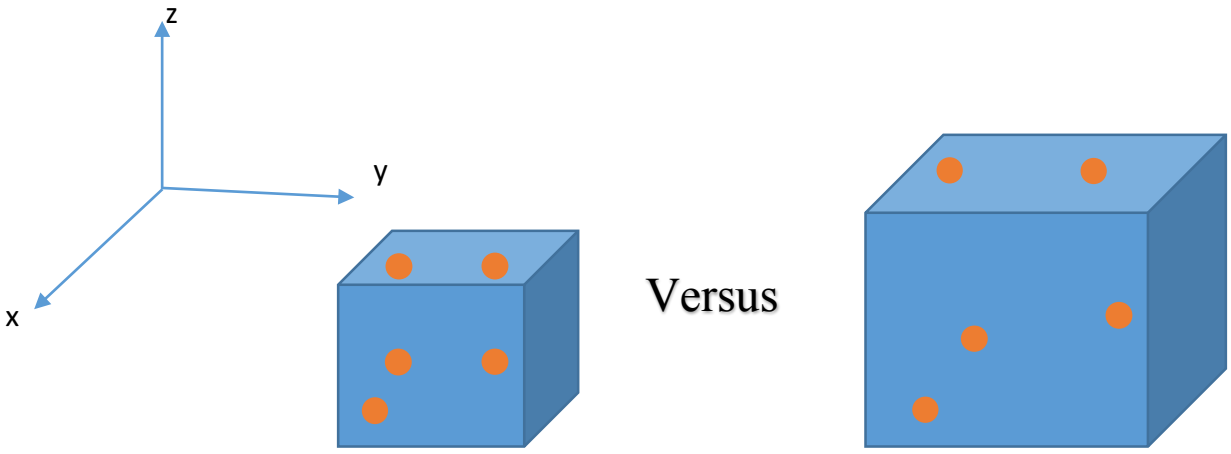

Figure 10: Differential Shrinkage: While the total number of the orange cells of interest (five) remain constant between the two pieces of tissue, the density is conditional on the relative shrinkage of the respective tissue slices. Extraneous variables including differential shrinkage and variable cortical thickness were controlled for by calculating the density of cells and estimating the total number of cells within the ROI.

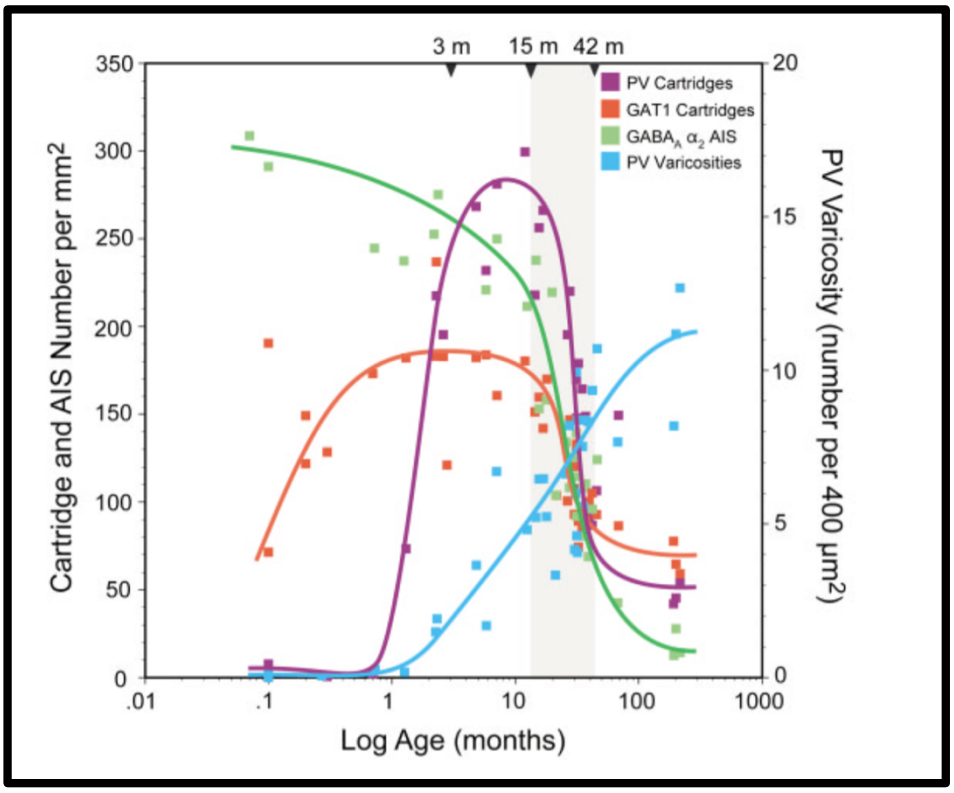

Figure 11: Developmental trajectory of GABAergic circuitry markers in the rhesus monkey PFC. Of particular interest for this project is the development of PV and GRα2 which have opposite trajectories. (From Cruz et al., 2003).

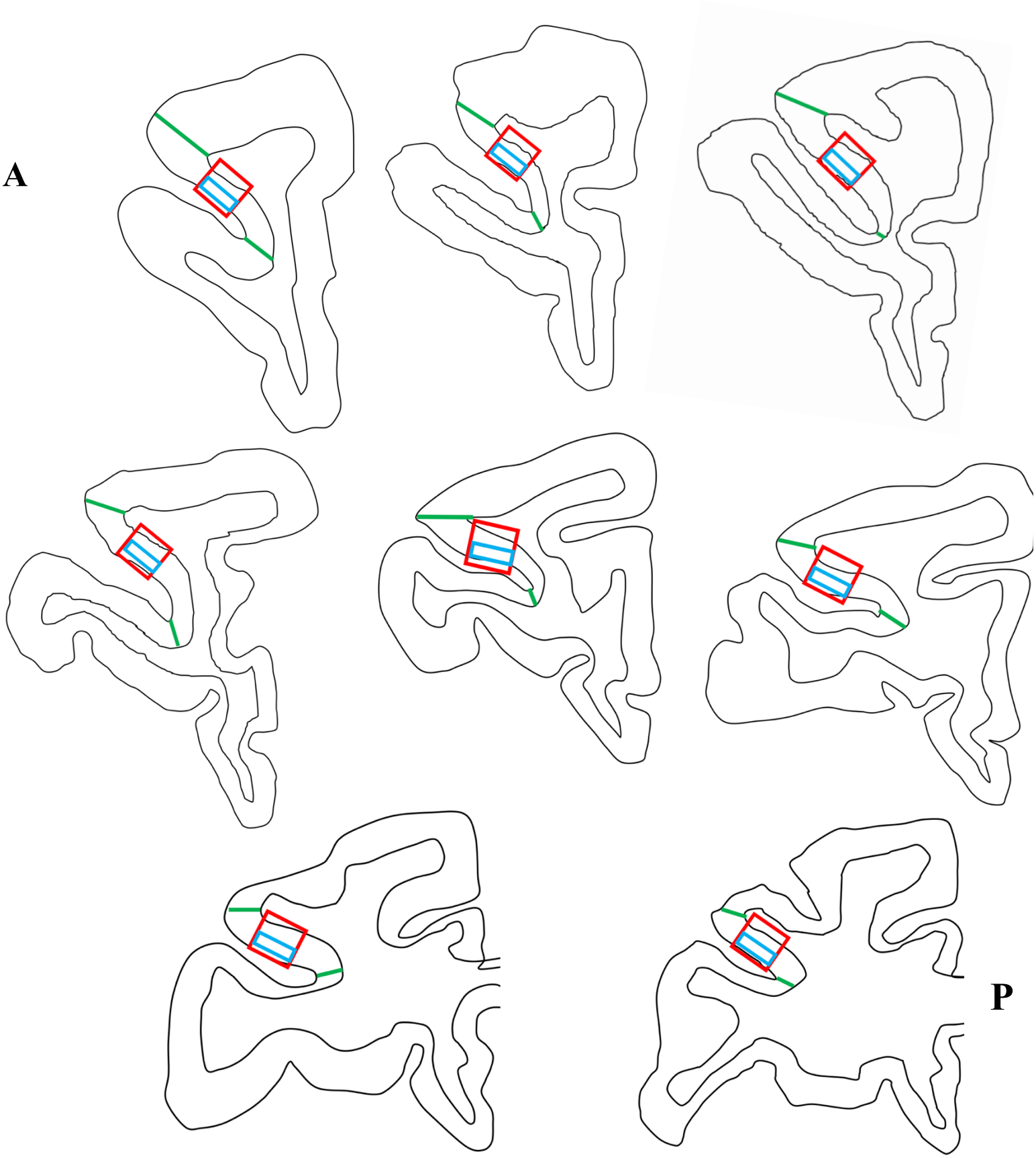
A
P

Figure 12: Images of a standard 1:40 section series used in analysis of PV-stained Rhesus monkey tissue through the dlPFC. The sections are arranged from anterior (A) to posterior (P). The Area 46, the upper bank of the principal sulcus, is demarcated by the two green lines on each outline. The region of interest, the middle 1/3 of BA 46, is represented by a red box and Layer IIIA is outlined in light blue. Counts were made in both hemispheres of each section.

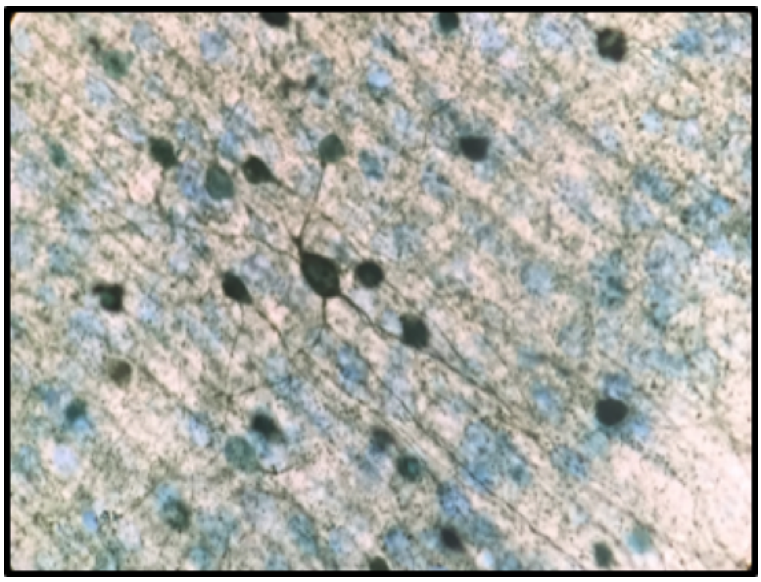

Figure 13: Parvalbumin-stained interneurons.

Figure 14: Stained Somatostatin cells. Numerous Antigen Retrieval techniques have thus far been unsuccessful in enhancing cell staining to the point that stereological counts can be performed. Here, two cells, with processes, are weakly stained above background levels.

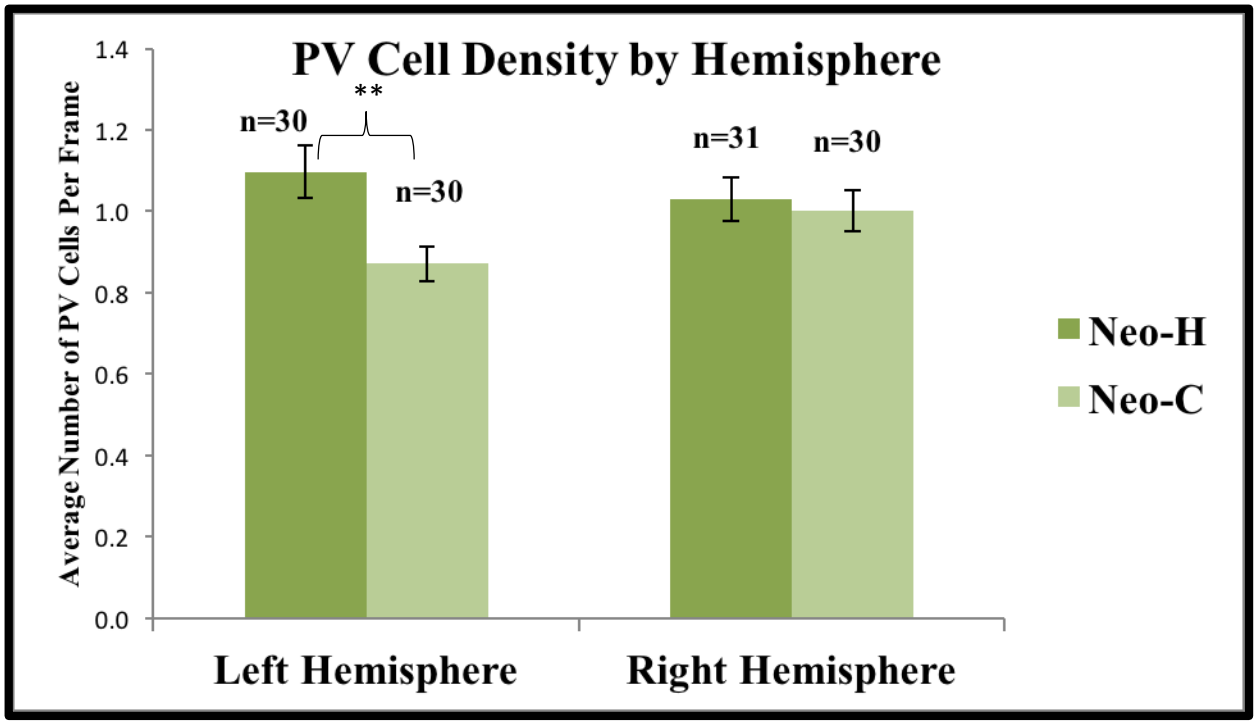

Figure 15: Analysis of the PV cell density showed a statistically significant (p = 0.0018) increase in the number of PV cells in the left hemisphere of Neo-H as compared to the Neo-C left hemisphere.

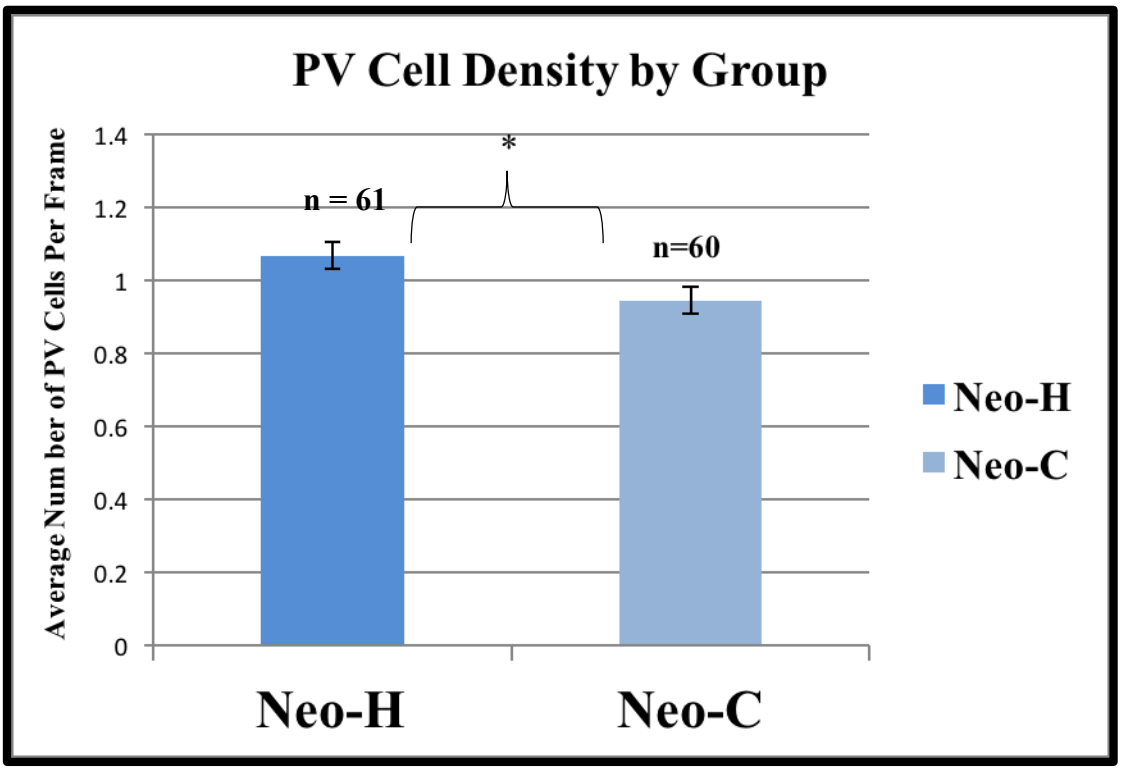

Figure 16: Analysis of the PV-cell density across groups showed a statistically significant increase in density within the Neo-H group as compared to the Neo-C group (p = 0.0177).

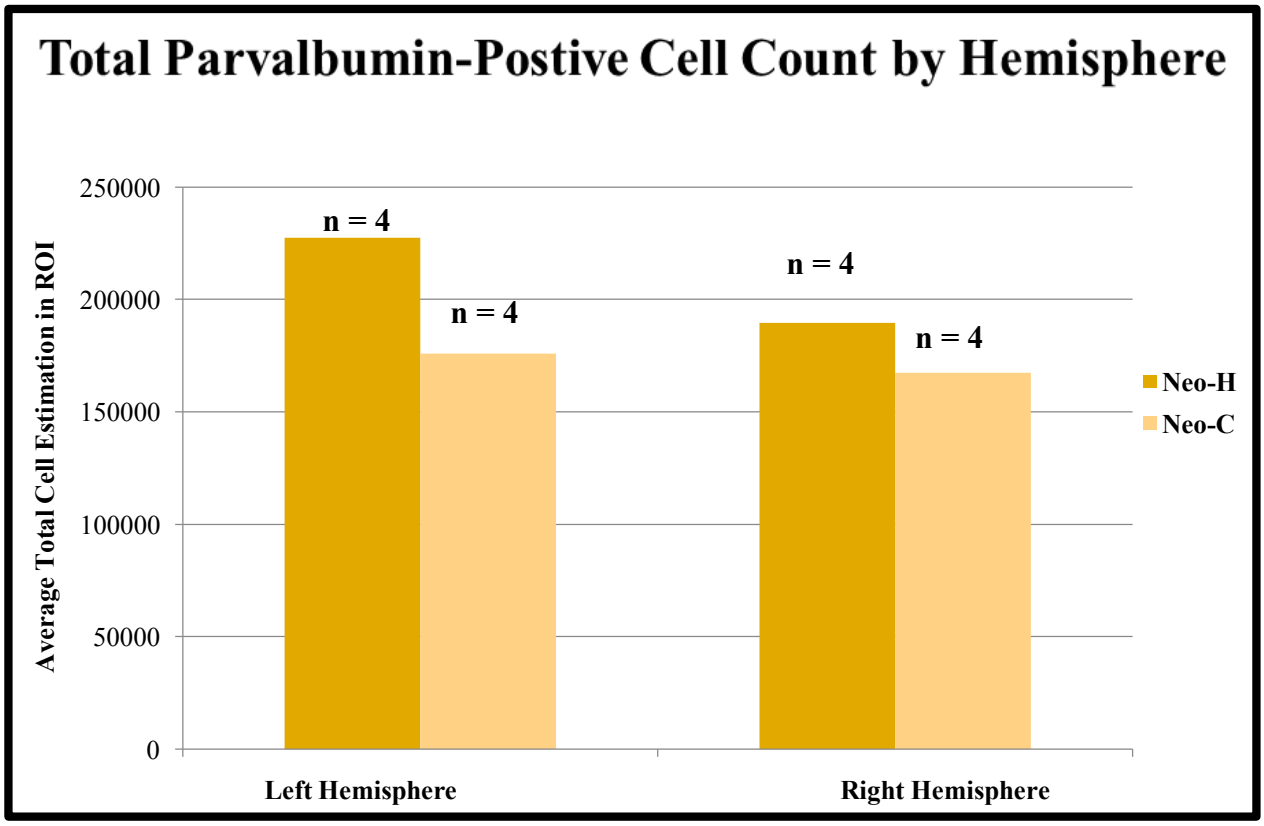

Figure 17: Confirming our density calculations, a qualitative analysis of the total PV-cell estimation within the ROI suggests an increase in the average number of cells in the left hemisphere of Neo-H as compared to Neo-C.

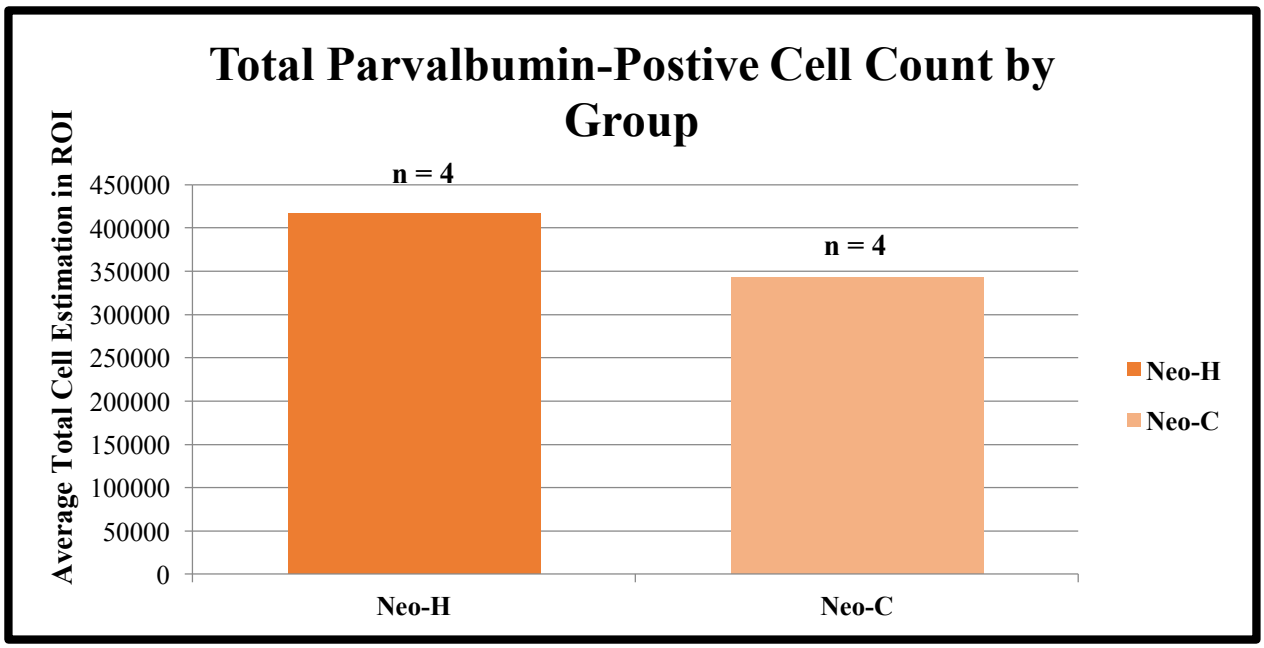

Figure 18: The average total number of PV-positive cells estimated were greater across the Neo-H group as compared to the Neo-C group.

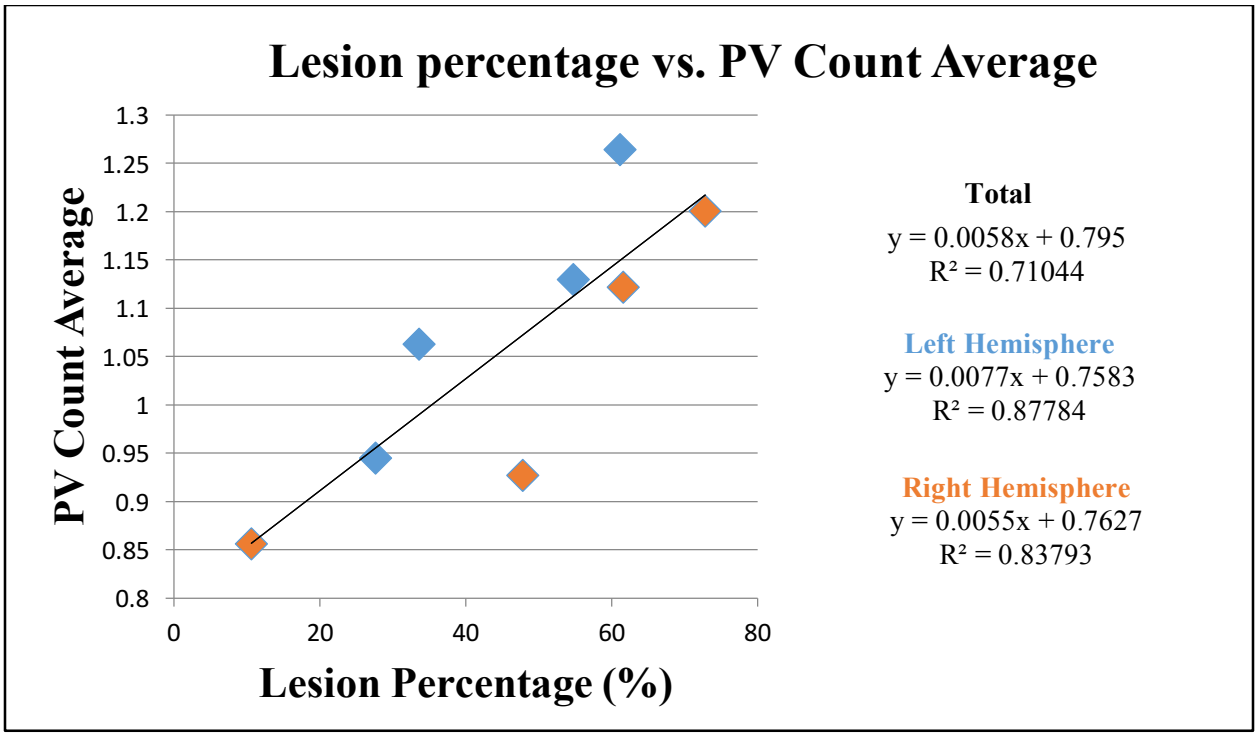

Figure 19: An analysis describing the relationship between percent reduction of hippocampus lesioned and PV density showed a strong positive correlation. When only the left hemisphere or right hemisphere lesions and densities were considered, there was a stronger positive correlation compared to the analysis of all lesioned hemispheres.

Totals	
Monkeys	8
Lesioned Monkeys ; Hemispheres	8 ; 4
Non Lesioned Monkeys ; Hemispheres	8 ; 4
Males	5
Females	3
Total Cells Counted	2681
Avg Cells Counted (Per Hemisphere)	167.6
Avg Cells Counted (Left)	1392
Avg Cells Counted (Right)	1289
Avg Cells Counted (Brain)	335.1
Total Counts	116
Total Counts (Neo-C)	55
Total Counts (Neo-H)	61

Figure 20: A summary of noteworthy dimensions within this study.

	Hemisphere Volumes	
	Neo-C	Neo-H
	0.1448	0.2044
	0.1362	0.1675
	0.1683	0.1853
	0.13025	0.14075
	0.1791	0.1675
	0.1406	0.1566
	0.1648	0.11745
	0.1355	0.13815
Average	0.14994375	0.15970625

Figure 21: The total estimated volume of each hemisphere was not greatly different between the Neo-C and Neo-H groups which lends additional support to our analysis of PV cell density.

Coefficient of Error	
A (H)	0.0258
B (C)	0.0285
C (H)	0.0257
D (C)	0.0339
E (H)	0.0344
F (C)	0.0326
G (C)	0.0336
H (H)	0.0314
Total	0.0307

Figure 22: The Coefficient of Error was determined using the Gundersen formulas (below). Monkeys are listed by case with group indicated by (H) for Neo-H and (C) for Neo-C. Here, Coefficients of Error are reported for each case as well as for the study as a whole. In all cases, the CE fell well below the commonly used 0.05 threshold.

Antigen Retrieval	
GRα2	SST
30 mins in Citrate buffer @ 80℃ followed by 45 mins in 2% NFDM	Distilled, store-bought water
75 mins in Citrate buffer @ 80℃ followed by 30 min in 1% NaBH4 and 45 mins in 2% NFDM	Six-well tray
30 mins in Citrate buffer @ 80℃with 45 min NFDM	60 min Citrate buffer @ 75℃, Tween, 10 mins in BloxAll
75 mins in Citrate buffer @ 80℃ with 45 min NFDM	60 min Citrate buffer@ @ 70℃, 10 mins in BloxAll, water from JB Lab
75 mins in Citrate buffer @ 80℃ with 45 min NFDM at high 1° concentration	Overnight Citrate buffer @ 70℃, weekend 1 incubation
60 mins in Citrate buffer @ 80℃, 30 mins in 1%NaBH4, and 45 mins in 2% NFDM @ three dilutions	45 min Citrate buffer @ 75℃, 10 mins in New BloxAll
60 mins in Citrate buffer @ 80℃, 30 mins in 1%NaBH4	
60 mins in Citrate buffer @ 80℃ with no Triton	
Distilled, store-bought water	
Distilled, store-bough water	
Overnight citrate, protease at @ 37℃ for 15 mins, humidified chamber, both floating and mounted tissue	

SySy
SCBT
Immunosta
Millipore

Figure 23: A breakdown of all the antigen retrieval manipulations carried out since Summer 2015. Because we did not not start SST until more recently, it has undergone fewer manipulations.

Col. title	Neo-H L hem	Neo-C L Hem	Neo-H R hem	Neo-C R hem	Neo-H Total	Neo-C Total
Mean	1.1044763	0.8714818	1.0291519	1.0012805	1.066196	0.942763
Standard deviation (SD)	0.3193	0.222	0.2689	0.2996	0.2947	0.2691
Sample size (N)	30	30	31	30	61	60
Std. error of mean(SEM)	0.0583	0.04052	0.04829	0.0547	0.03774	0.03474
Lower 95% conf. limit	0.9852	0.7886	0.9305	0.8894	0.9907	0.8732
Upper 95% conf. limit	1.224	0.9544	1.128	1.113	1.142	1.012
Minimum	0.4054	0.5	0.32	0.4	0.32	0.4
Median (50th percentile)	1.132	0.8481	1.05	1.119	1.097	0.8889
Maximum	1.75	1.36	1.476	1.765	1.75	1.765
Normality test KS	0.1195	0.1297	0.1248	0.1428	0.09991	0.08421
Normality test P value	>0.10	>0.10	>0.10	<0.10	>0.10	>0.10
Passed normality test?	Yes	Yes	Yes	No	Yes	Yes

Figure 24: Statistical calculations for comparisons of PV cell density within each hemisphere and across Neo-H and Neo-C groups using GraphPad InStat. Significant differences were found between the Neo-H and Neo-C groups as well as between the left hemispheres of both the lesion and control cases.

Lesion Animals		Left Hemisphere	Right Hemisphere	Monkey
Case A	E3	265947.7	229945.5	495893.2
Case C	C2	286853.2	206875.2	493728.4
Case E	D4	193785.7	164048.6	357834.8
Case H	F3	162430.0	156787.0	319217.0
Neo-H Animal Averages		Left Hemisphere (Avg)	Right Hemisphere (Avg)	Monkey
		227254.2	189414.1	416668.2

Control Animals		Left Hemisphere	Right Hemisphere	Monkey
Case B	F1	150858.5	156133.5	306992.0
Case D	E2	162690.9	184105.5	346796.3
Case F	C1	207313.3	183128.8	390442.1
Case G	G 4	183024.1	146425.2	329449.3
Neo-C Animal Averages		Left Hemisphere (Avg)	Right Hemisphere (Avg)	Monkey
		175971.7	167448.2	343419.9

Figure 25: Estimations of total PV-positive stained cells across hemispheres and cases in both Neo-H and Neo-C groups. In all cases, more cells were estimated in the Neo-H cases as compared to Neo-C cases, confirming our PV density results.

Case Number	Monkey Name	Left Hemisphere Lesion Extent by % Damage	Right Hemisphere Lesion Extent by % Damage	Average Damage to Both Hemispheres (%)	Weighted Average Damage to both Hemispheres (%)
Neo-H-ibo-1	Baba-ghanoush	63.8	2.9	33.2	1.8
Neo-H-ibo-2	Tostito	54.4	80.9	67.6	44.0
Neo-H-ibo-4	Jeep	20.3	67.3	43.8	13.6
Neo-H-ibo-5	Huron	20.7	84.0	52.6	17.5

Figure 26: Note: Values reported in Heuer and Bachevalier 2011. Weighted average is (%L x %R)/100.

Case Number	Left Hemisphere % Volume Reduction	Right Hemisphere % Volume Reduction	Average % Reduction
Neo-H-ibo-1	27.6	10.6	19.1
Neo-H-ibo-2	61.1	72.8	67.0
Neo-H-ibo-4	33.6	61.6	47.6
Neo-H-ibo-5	49.1	64.0	56.6

Figure 27: Note: Values reported in Heuer and Bachevalier 2011.

Case Number	Weighted Average Damage to both Hemispheres (%)	Session-Unique Delayed Nonmatching-to-Sample Task (Error/Trial #) (5 sec, 30 sec)		Total Errors (Object Self-Ordered Task)	Perseverative Errors (Object Self-Ordered Task)
Neo-H-ibo-1	1.8	X	25	35	29
Neo-H-ibo-2	44.0	13.3	27.5	46	63
Neo-H-ibo-4	13.6	15.0	50	43	42
Neo-H-ibo-5	17.5	27.6	X	49	42

Figure 28: Note: Values reported in Heuer and Bachevalier 2011. These numbers represent the number of errors/trials it took each monkey to reach the learning criteria (information maintenance). "X" represents 0 trials.

CE Equations (Altunkaynak, 2012)

1. Variance due to Noise

$$Noise = 0.0724 \times (b/\sqrt{a}) \times \sqrt{n \times \sum P}$$

Where a = area from Canvas
b = perimeter from Canvas

2. Variance due to Systematic Random Sampling

$$VAR_{SRS} = \frac{3(A - s^2) - 4B + C}{12}, m = 0$$

$$VAR_{SRS} = \frac{3(A - s^2) - 4B + C}{240}, m = 1$$

$$A = \sum_{i=1}^{n} (Q_i^-)^2$$

$$B = \sum_{i=1}^{n-1} Q_i^- * Q_{i+1}^-$$

$$C = \sum_{i=1}^{n-2} Q_i^- * Q_{i+2}^-$$

Where Q indicates ordered counts
s^2 = Noise

3. Total Variance

$$TotalVar = s^2 + VAR_{SRS}$$

4. Gundersen Coefficient of Error

$$CE = \frac{\sqrt{TotalVar}}{s^2}$$

5. Effect Size

$$r = \frac{Z}{\sqrt{N}}$$

Where Z = Z score
N = Total number of samples

Supplemental Writing

Other GABAergic Alterations in Schizophrenia

While parvalbumin was the most important neurotransmitter explored as part of this research, other components of the GABA system were also selected as objects of investigation. GABA Receptor Alpha 2 Subunit (GRA2), seen in cartridges along the axon initial segment, increase in levels within schizophrenia patients possibly via an upregulation mechanism in response to decreased GABAergic input (Charych et al. 2009). The axon initial segment (AIS) is the structure responsible for integrating all the information that a neuron receives via its synapses to produce, or not produce, an action potential. Morphologically, this is the stretch of axon between the axon hillock, which is rich in Na^+ channels, and the beginning of the myelin sheath (Safronov, 1999; Clark, 2009). Research involving schizophrenia patients revealed increased GRα2 within the PFC, hippocampus and anterior cingulate gyrus, while additional research found increased alpha-1 subunit levels in BA 9,10, and 11 of patients (Benes 1992, 1996 and Ohnuma, 1999).

Previous research suggests that somatostatin mRNA is reduced in patients with schizophrenia (Morris, Hashimoto and Lewis, 2008). Martinotti cells, multipolar neurons with short branching dendrites, can express either SST or Calbindin (Sugino, 2006). They target the distal apical dendrites of pyramidal neurons (Gonchar et al., 2002), resting primarily in layer II, IIIA and V, in rats. Martinotti cells are located within the deep layers and have axons that ascend to the cortical surface. They are excited by local pyramidal cells and provide inhibitory feedback (Smiley et al.). According to Gonchar et al. (2002), SST neurons synapse on somata, dendrites, spines and the AIS, less densely innervating than PV, suggesting that they may influence the excitation as well as the initiation of excitatory outputs by pyramidal neurons. According to

Hicks et al. 1998, SST may work by activating postsynaptic potassium channels through SST receptors, counteracting depolarization of the pyramidal cell. In general, fewer SST cells are present, and innervate to a pyramidal cells to a lesser degree, as compared to PV ones (Rudy, 2013).

Furthermore, calbindin, a calcium binding protein which under normal physiological conditions plays a role in calcium buffering and sensing, has been shown to be dramatically decreased in number in patients diagnosed with schizophrenia (Beasley, 2002 and Conde, 1994). More recent research has shifted emphasis from Calbindin in favor of other neurotransmitters noted above, namely SST (Lewis and Hashimoto, 2007).

GAD is another component of the GABAergic circuitry that is affected in humans with schizophrenia. That said, the deficit in GAD in these patients appears to be isolated to the prefrontal cortex and to only GAD-67. GAD 65 and total levels of mRNA GAD appear to be unaffected (Volk et al 2000). Lower levels of prefrontal GAD, in both RNA and protein form, have been correlated with lower GABA concentrations, less GABA release, lower levels of GAT-1 and up-regulation of $GABA_A$ sites (Benes et al., 1992, Volk, 2000, Volk 2001).

Furthermore, the GABA transporter 1 (GAT-1), which lowers synaptic GABA levels by removing the neurotransmitter from the synaptic cleft, appears to exist at lower levels in layers II-VI of Brodmann areas 9 and 46 within humans with schizophrenia (Volk, 2001; Woo, 1998). While there is no total reduction of GAT-1 in the PFC there is likely a reduction in chandelier GABAergic cells which would suggest reduced inhibition by chandelier cells onto the AIS of pyramidal cells. GABA transaminase the principal catabolic enzyme for GABA in mammalian brains does not show a significant reduction in patients with schizophrenia.

GABA

While this study considered only a few of the many markers associated with GABA transmission in the frontal region of the brain, there are several other aspects of GABA circuitry that are important to understand. To begin, there exists at least two isoforms of the major synthetic enzyme, GAD or glutamate decarboxylase, which are named after their respective molecular weights measured in kiloDaltons, GAD 65 and GAD 67. GAD 67 has a relatively short half-life and appears to be generally responsible for nonvesicular GABA release (Fenalti, 2010). More specifically, GAD 67 is involved primarily in the activity of the D2 class of dopamine receptors, which play a significant role in motor control by the basal ganglia (Soghomonian and Martin, 1998). In contrast, GAD 65 is generally less physiologically available, although it has a longer half-life than GAD 67. GAD 65 is primarily responsible for vesicular GABA release and predominantly involved in the activity of the D1 class of dopamine receptors (Soghomonian and Martin, 1998).

Furthermore, there are four primary forms of transporters specific to GABA. While GAT-2 is primarily involved in functions unrelated to the nervous system, GAT-1 and GAT-3 play a major role in neuronal firing. In order to limit its impact on a given pyramidal cell, GABA is transported out of the synaptic cleft by the sodium- and chloride-dependent GAT-1, the primary GABA transporter (Zhou, 2013). GAT-3 serves a similar function but uses sodium electrochemical gradients (Schlessinger, 2012). Finally, vGAT is also expressed in the brain and is believed to be primarily responsible for shuttling GABA into presynaptic vesicles (Chaudhry, 1998).

Within humans, GABA is involved in the development of the nervous system and for many functions early in life including neuronal excitability, maintenance of oscillatory activity,

and neuronal plasticity (Kilb, 2012). The development of neocortical GABAergic interneurons in humans and monkeys arises from intra-cortical sources while the interneurons of the rat brain are primarily extra-cortical, derived from dorsal pallium (Kilb, 2012; Al-). Most GABAergic interneurons are functionally developed by early puberty at which time nearly all are inhibitory, with some shifting from a previously excitatory state (Kilb, 2012). Furthermore, there exists a simultaneous shift in excitatory neurotransmission such that the shift it GABAergic circuitry may be compensatory (Kilb, 2012). While GABA may generally follow certain developmental trajectories, different interneuron types should be analyzed separately in order to be as thorough as possible.

Histological Processing: GRα2 and Somatostatin

Normally, a new antibody is run at several dilutions simultaneously, using levels suggested by the manufacturer as well as those published in the literature, in order to get a strong sense of how well the antibody adheres to specific tissue. When even strong dilutions are insufficient to reveal clear, specific staining other methods, including antigen retrieval, (see Figure #) can be used in hopes of visualizing the stain. For example, the somatostatin (Immunostar and Millipore), and GABA receptor alpha 2 subunit (Synaptic Systems and Santa Cruz BioTech) antibodies did not produce the desired staining at a variety of dilutions including those suggested by the manufacturer and those published. In an attempt to navigate this issue, our lab investigated several methods of antigen retrieval. Slides stained for GABA receptor alpha 2 and somatostatin underwent Heat Induced Epitope Retrieval (HIER) and Proteolytic Induced Epitope Retrieval (PIER) in order to create a better epitope binding site for the antibody (see Figure #).

The first form of antigen retrieval used by our lab was HIER. This method is characterized by the use of a sodium citrate buffer in conjunction with heat treatment. Specifically, our buffer solution was a 10mM Na^{2+} citrate solution made using tri-sodium citrate. The pH was adjusted to 6.0 using a 1N HCl solution. Additionally, the nonionic surfactant Tween 20 was incorporated into the solution at 0.05% in an attempt to reduce the amount of nonspecific binding of antibody and subsequent staining. Tissue was heat-incubated in this solution for between 45 minutes and overnight. The temperature of the solution was kept at a constant level throughout incubation, which ranged from 70°C to 95C°. While tissue was stained to a far greater extent, none of the manipulations resulted in the adequate staining of relevant structures. In the case of the Millipore SST, some somatostatin-positive cells could be identified (see Figure #), albeit at a levels too low to count using our stereological techniques. The HIER antigen retrieval only increased background noise in the SCBT somatostatin and the two GRα2 antibodies.

In addition to HIER, our lab also explored the PIER method of antigen retrieval in an attempt to visualize the GRα2 antibody. Specifically, we used the protease form of PIER, at a concentration of 0.05% in solution, though other proteolytic enzymes including trypsin and pronase may be used similarly. While this method is normally used on pre-mounted tissue, our lab is better equipped for running IHC on free-floating tissue. Thus, we performed two simultaneous attempts of the PIER method, one in which we incubated free-floating tissue in the protease solution and another in which the solution was pipetted directly onto mounted tissue. As is customary, the slide-mounted tissue was incubated within a humidified chamber in order to prevent tissue desiccation. In both instances, tissue was incubated at 37°C as is standard, for between 5-15 minutes whereby free-floating tissue was exposed to solution for less time because

of its more direct interaction with the enzyme. The free-floating tissue appeared to be more darkly stained than its control counterpart but no relevant structures were visible. The slide-mounted tissue appeared to be well-stained, but the method proved to be too harsh, in conjunction with our IHC protocol, such that the tissue was too damaged to be analyzable.

Antigen Retrieval

Although we obtained excellent staining of PV cells, unfortunately our attempts to visualize the SST and GRα2 have been unsuccessful thus far. While the quantitative results of this project relate exclusively to the analysis of parvalbumin cells, a considerable effort was invested in attempting to visualizing poorly stained antibodies through antigen retrieval. Antigen retrieval is a technique used to disrupt protein crosslinks resulting from the fixation process and allow antibodies to bind epitopes. Because of its relative popularity among antigen retrieval methods, we first tried the Heat-Induced Epitope Retrieval (HIER) method. Specifically, we used the citrate buffer method, which is designed to break the protein crosslinks that prevent antibody binding by heating the sections within a buffer solution (IHC World). When this basic protocol was unsuccessful we tried a variety of other manipulations. For example, we used non-fat dry milk as a blocking agent but when this manipulation did not generate the desired staining we altered additional variables. Because IHC in our lab had previously been affected by water, we used store-bought distilled water as well as water from the Bachevalier Lab (Table 4). In addition, we used the Proteolytic-Induced Epitope Retrieval (PIER) which is based on similar reasoning as the HIER method, but is slightly harsher on the tissue as it uses proteolytic enzymes to break down the protein crosslinks (IHC World; Figure 7).

Somatostatin Staining

While Somatostatin remains a key marker of interest in the GABAergic circuitry story, it ultimately proved elusive for the sake of this project. Oddly, the small number of seemingly random cells we have been able to visualize were fully stained. We expect that we will eventually visualize this cell type, which synapses on distant dendrites and represent a specific, and integral component of distal inhibition, far from the soma of the pyramidal cell (Lewis and Hashimoto, 2007)(see Figure 9).

GABA Receptor Alpha Two Subunit Staining

Similar to the SST staining, we encountered quite a bit of unresolved difficulty when it came to staining for the GABA receptor alpha two subunit. Unlike SST, the two AR methods were unable to aid in the selective staining of even a small number of structures. One potential reason for this is the relative thickness of our tissue, 50 μm, as well as the use of antibodies not yet shown to be successful in rhesus monkey tissue. Visualization of the GRα2 subunit would allow us visualize cartridges on the AIS of pyramidal cells, a key site for the regulation of action potentials, known as spatial summation (Nie, 2009; see Figure 9).

Coefficient of Error

The Gundersen CE is primarily determined by the Total Variance across all sections calculated, which itself is the combination of both the Variance Due to Noise and the Systematic Random Sampling Variance (SRS Variance). The Variance Due to Noise, formerly the Nugget Variance, is a measurement of the intra-sectional variance, such that a value that is too high requires more sampling within given sections. Conversely, SRS Variance is a measure of inter-sectional variance and a high CE requires more sections be sampled (StereoInvestigator 8.0). A smooth contour between different regions could be assumed, in comparison to a more randomly

distributed surface, as in the case of a nugget. Thus, the m = 1, as opposed to m = 0, version was used in calculating the Variance due to Systematic Random Sampling, a distinction that determines the denominator for this formula (Coefficient Theory; see Equations). Ideally, the SRS Variance and the Variance Due to Noise will be relatively similar, although this is not something we measured (Stereo Investigator 8.0).

Stereology

Stereology, as generally defined in neuroscience, is a process by which three-dimensional analyses may be conducted given only two-dimensional information, unbiased by the shape, size or orientation of the object. Stereology utilizes systematic, random sampling in order to achieve the most unbiased count estimates taken from a known fraction of the entire object of interest. Two of the most popularly used features of stereology include the optical disector and the optical fractionator technique, both of which are solely implemented on relatively thick tissue, as opposed to very thinly sliced tissue, to allow for counting in three dimensional space.

The optical fractionator technique can yield measurements of both density as well as the total number of a given object of interest, using a set of unbiased virtual counting spaces that sample an entire region of interest. These virtual counting spaces are unbiased in that they begin from a random point and exist at a uniform distance between individual spaces in the X and Y plane (Optical Fractionator, online). On the other hand, the optical disector works by focusing through tissue in the Z-plane and counting the number of new objects that come into view (Optical Disector, online; Ward, Rosen, and Von Bartheld, 2008). The distance of Z-plane, which the field of focus is moved through can be measured by a position encoder on the microscope. At their foundation, both methods work to ensure that all objects are only counted once, even if they were cut as part of tissue slicing.

A measurement of the density of a specific marker requires the calculation of the area and volume of the region of interest, in this case the portion of Layer IIIA of the dlPFC that falls within the middle ⅓ of the upper bank of the principal sulcus. This definition was helpful since there are often no clear boundaries that can be used in counting this area of Layer IIIA. Furthermore, although we used a total of only eight monkeys as a part of this study, our number of counts were consistent with other stereological research performed in cerebral cortex (Scheaffer, 1996). Other studies employing the same stereological techniques used a similar number of sections and counts, approximately 10-20 per section, in order to calculate unbiased estimates (Geinisman, deToledo-Morrell, Morrell, Persina, and Rossi, 1992; Christensen 2007; Morecraft 2013). Thus, our stereology procedure was consistent with the current body of literature.